Establishing BRET assays to investigate the protein-protein interaction between transcription factor-cofactor complexes. An approach to develop small molecule inhibitors

Final Report for the Austrian Marshall Plan Foundation

Autor:
Florian Kabinger

Supervisor home university:
FH-Prof. Dr. Thomas Czerny

Supervisor host university:
Angela N. Koehler, PhD

Date
30.04.2020

Abstract

Transcription factors (TFs) present highly promising targets for future drug development. During the past decades TFs were shown to play important roles in physiological and pathological processes including the onset and progression of cancer. One of these key regulatory factors is c-Myb, a sequence specific TF that is involved in a myriad of cellular pathways. Its activity is tightly linked to the regulation of proliferation and differentiation. Moreover, c-Myb was shown to be a potent proto-oncogene that is frequently deregulated in hematopoietic malignancies. Recent studies revealed that c-Myb relies on a complex network of protein-protein interactions (PPIs) together with its cofactors. Disruption of the interaction between c-Myb and TAF12 using a peptidomimetic demonstrated potent and highly specific effects against leukemia cells. The aim of this project was to build on these insights and advance chemical probe development against the PPIs of c-Myb´ s interactome. Unfortunately, TFs are very challenging to target and were even described as “undruggable” until recent years since conventional approaches to develop inhibitors failed broadly. Thus, innovative techniques such as Small Molecule Microarrays (SMM) and Bioluminescence Resonance Energy Transfer (BRET) assays were applied to find small molecules with the desired features. Within the scope of this thesis it was possible to successfully establish and apply BRET assays focusing on the interactome of c-Myb. Thereby, we were able to nominate a small molecule probe, named TM1, which putatively modulates the interaction of c Myb : TAF12. In accordance with this discovery we revealed a number of intriguing TM1 mediated biological effects including dose dependent degradation of c-Myb and potent anti-cancer effects. The presented results are encouraging and will potentially lead to the nomination of a high-quality small molecule probe, which can be further used as starting point for the development of cancer therapies.

Table of Contents

Introduction

Transcription of genetic information into mRNA which can be later translated into proteins, presents one of the most impactful procedures in living organisms [1]. The regulation of transcription is a highly complex and tightly coordinated system that involves more than 1500 factors [3]. Simplified, the regulation of transcription can be described as the central control unit of every cell since it is the underlying course why hepatocytes and cardiac muscle cell can have the same genetic information but very different phenotypes.

One of these key regulatory factors is c-Myb, a sequence specific transcription factor (TF) that plays an important role in the regulation of proliferation and differentiation and is essential for the development of the human hematopoietic system [4]. Moreover, deregulation of c-Myb is frequently observed in a large number of cancer types, suggesting that c-Myb regulated genes are critical for the formation of different cancer types [5–9]. Recently, the importance of c-Myb as an oncogene was supported by the publication of dependency maps that revealed that c-Myb is a strongly selective dependency of hematopoietic malignancies [10,11]. Despite extensive research that provided intriguing insights into the biology of c-Myb, the molecular complexity how c-Myb regulates different transcriptional programs is still not fully understood. It was shown that the activity of c-Myb is regulation at a variety of steps ranging from alternative splicing, over protein-protein interaction networks to post translational modifications [6]. Thus, c-Myb can have very diverse functions in different cell types, depending on a myriad of influencing pathways [5,6].

A recent publication from Chris Vakoc and coworkers has impressively underlined the potential of targeting c-Myb and its interactome. It was shown that c-Myb forms a protein-protein interaction with TAF12, a subunit of TFIID complex. Functional blockage of this interaction with a squelching peptide caused potent anti-leukemia effects [12]. Concise, this suggests that small molecules that block key protein-protein interactions of c-Myb and cofactors could be a potent therapeutic approach. However, chemical probes with the defined features are required to address this potential. Unfortunately, to this date very few putative Myb targeting chemical probes are known.

Due to the complexity of TFs and the underlying molecular mechanisms it remains extremely challenging to develop high quality small molecule probes against TFs. However, over the last 20 years impressive progress was made to deconvolute the complexity as well as to tackle the undruggability of mentioned targets [13–15]. The goal of this master thesis project was to build on this progress in order to nominated, characterize and develop small chemical probes against the specific transcription factor c-Myb. Chemical probe development for c-Myb has been a goal for Angela Koehler´s research group

since years. This is the reason why extensive groundwork and profound expertise could be utilized to successfully complete the project.

The following chapter will start with a brief introduction about the general biology of transcription and the specific role of c-Myb. It will continue with a critical analysis of the challenges and opportunities of transcription factors as drug targets and will end with a description of the excellent groundwork that was provided.

The biology of transcription and transcription factors

Transcription can be defined as the process of RNA synthesis based on DNA encoded information. More specific, a DNA dependent RNA-Polymerase (Pol) synthesizes an RNA strand that is complementary to the DNA template strand [1]. In eukaryotic cells three different DNA dependent RNA-Polymerases are used. Pol I and Pol III are utilized for the synthesis of rRNAs and tRNAs, respectively. Pol II is essential for the synthesis of long noncoding RNAs and especially mRNAs, which are later translated into proteins [2]. Because of the focus of this thesis on chemical probe development against proteins, only Pol II mediated transcription will be discussed.

Pol II is the consistent key player in the expression of protein coding genes since it is the only known enzyme capable of synthesizing mRNA [2]. However, a complex network of additional factors, so called transcription factors (TF) is essential to successfully transcribe a specific gene. Thereby TFs fulfill a variety of functions including the assembly of large protein complexes and enzymatic activities [3,16,17]. In order to develop chemical probes that artificially regulate transcription it is fundamental to understand the concept of TFs and the interplay between TFs, Pol II and chromatin.

All TFs have the ability to control the rate of gene expression, since it is the defining feature of TFs [3]. In addition, many TFs contain a DNA binding domain (DBD) which enables them to bind sequence specific to DNA [2]. In vitro assays have revealed a so-called consensus sequence for a number of well-studied TFs [18]. However, it is noteworthy that the ability of TFs to bind directly to DNA is used contradictory in the literature. This confusion is mainly caused by the dual use of the term “factor”. It is used for single protein transcription factors, like Myb, and for large protein complexes, exemplified by the Transcription factor II D (TFIID), a complex of 14 proteins. For both types of “factors” it was demonstrated that they can interact with DNA in a sequence specific manner [19,20]. However, adding direct protein-DNA interaction as an essential feature of TFs would mean that several subunits of TFIID would not meet the criteria and would consequently not be classified as TFs. Recent publications suggest that a more accurate definition would include that TFs have the ability to control the expression of a gene and bind direct or indirect (*via* protein-protein interaction) to DNA [21]. This clarification highlights the importance of the network of protein-protein interactions and is widely

applicable. Because of the emphasis of this work on chemical probe development for TFs it is crucial to distinguish if a small molecule targets a single protein or a complex. Thus, the described clarification will be applied throughout the thesis.

Another layer of complexity is added to the discussion of TFs by the fact that the transcription of different genes requires a set of similar TFs, so called "general TFs", and a set of "specific TFs" [1,2]. Although, general TF (complexes) show slight variation in the composition of subunits they are generally essential for the expression of a gene. In contrast, specific TFs are unique for transcriptional programs, that are for example limited to a specific cell type [3].

The molecular mechanism of transcription

Pol II mediated transcription of a gene can be classified into three phases. The first phase is called initiation whereat the Pol II needs to find the beginning of gene and initiates the synthesis of mRNA. In the second phase, elongation, the mRNA is actually synthesized while Pol II travel through the gene. The last phase, termination, is characterized by the disassembly of the transcription complex and the release of the final mRNA [2]. The focus of this introduction will be laid on the initiation phase. It is coordinated by a highly complex network and is the crucial points of regulation of transcription [1]. Thus, providing interesting targets to artificially control the expression of a gene [22].

To start transcription of gene Pol II must find and bind the beginning of gene which is called promotor [2]. Pol II itself does not bind to DNA in a sequence specific manner, thus it requires a set of TFs that mediate this process [23]. Promotors consist of a variety of sequence elements that reflect consensus sequences and enable thereby binding of TFs [2,18]. Eukaryotic promotors are highly diverse which makes it difficult to define a consistent organization. However, several conserved sequence elements were frequently found in functional promotors [24].

Generally, promoters can be divided into a core promotor region, proximal promotor elements and distal regulatory elements. The core promotor flanks the transcription start site (TSS) and contains the binding sites for general transcription factor (e.g. TATA box). Thus, core promotors are sufficient to recruit Pol II and to induce basal transcription of a gene. Proximal promotor elements are directly adjacent upstream to the core promotor [24]. Concise, proximal promotor elements contain the binding sites of specific TF and are therefore used to control the level of transcription. Distal elements have the same function as proximal promotor elements but can be several Mb away from the core promoter, as the name suggests. To span the distance, DNA loops are formed which enable proteins that are bound at distal elements to directly interact with the core transcriptional machinery. Moreover, in many cases a mediator complex is present which bridges proteins bound to distal elements, specific TFs and the core transcriptional machinery [2].

It is noteworthy that the DNA is present as chromatin instead of freely accessible DNA. Chromatin is a packaged form of DNA that consists of the DNA itself bound by several types of conserved proteins including histones. Accessibility of chromatin for TFs and Pol II in promotor regions is tightly regulated by post translational modifications of those histones [2]. This is another key mechanism for transcriptional regulation that has raised attention in the field for chemical probe development [25].

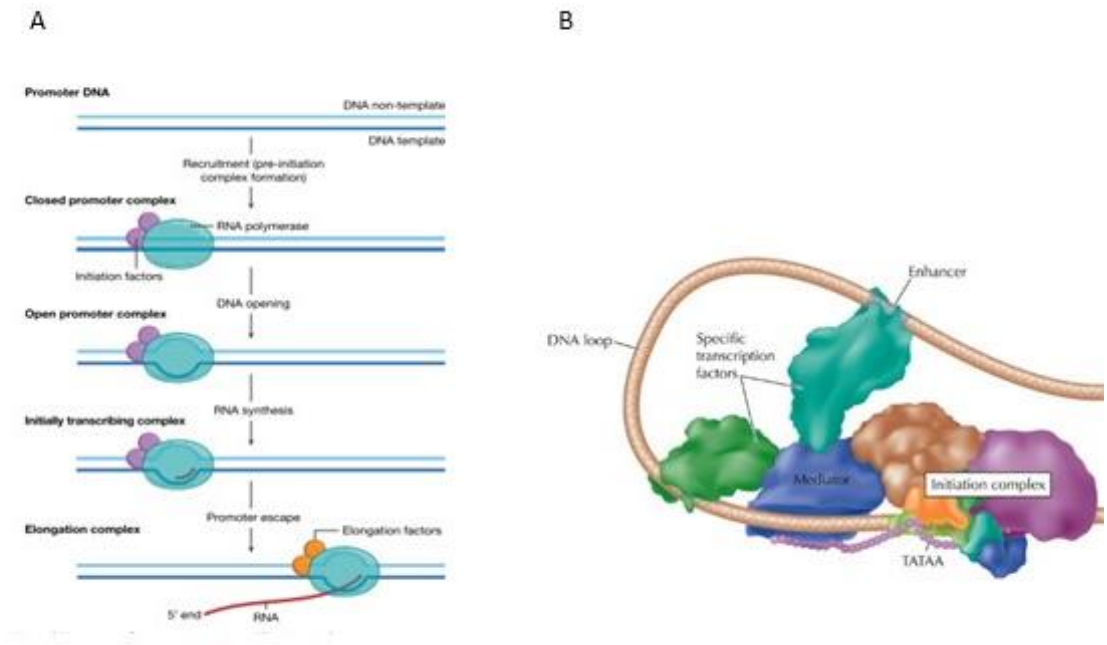

Figure 1: **The biology of eukaryotic transcription** a) Key steps of gene transcription, adopted from Cramer, P. [1] ; b) The interplay of specific and general TFs during the initiation phase of transcription adopted from the Molecular Biology of the Cell, 4th edition [2]

The biology of c-Myb and its interactome

The discovery of c-Myb

MYB genes are a large family of genes that encode functional diverse proteins with a conserved DNA binding domain as common feature. MYB gene products play important roles in a variety of eukaryotes including humans and plants and are even found in viruses [8,26]. The viral Myb protein v-Myb was the first family member that was discovered and presumably gave the whole family its name, MYB which stands for MYeloBlastosis. In the 1980s v-Myb was first described as a potent oncogene of the avian myeloblastosis virus (AMV) [27]. This virus is a retrovirus that can induce myelomonocytic leukemia in chickens. Interestingly, it was very early observed that AMV can replicate in myeloid cells and fibroblasts in culture, but that it could solely transform myeloid cells [8]. This is striking since up to this day the function of Myb proteins seems to be highly dependent on the cellular environment [6]. Shortly after the discovery of v-Myb its human ortholog c-Myb was described [19]. Later two more paralogous of c-Myb that contain the same conserved DNA binding domain were found in the human genome and

were called A-Myb and B-Myb, respectively [8]. Notably, all human gene products of the MYB family are involved in the regulation of proliferation and differentiation [4]. A more detailed comparison of the different proteins will be provided in the next paragraph by means of their domain structure.

Comparison of Myb family members and their domain structure

All vertebrate Myb related proteins share a conserved DNA binding domain (DBD) that consists of three imperfect 52-53 amino acid repeats, called R1, R2 and R3 [28,29]. Extensive research was performed to elucidate the structure, function and consensus sequence of such DBDs. Each repeat consists of three helices containing crucial tryptophan residue, which seems to be essential for the formation of the hydrophobic core of each helix. Bound to DNA, helix two and three form a helix turns helix (HTH) motif, that contains the characteristic recognition helix. Interestingly, only R2 and R3, also known as the R_2R_3 minimal DBD, are required for binding to the DNA consensus sequence. R1, which is present in all vertebrate Myb proteins but not in v-Myb, does not interact with DNA specifically [28,29]. In accordance with the described structure, a consensus sequence was found for the R_2R_3 minimal DBD. The sequence YAACNGHH is bound by the recognition helix of R2 and R3 of every Myb related DBD and is therefore called Myb responsive element (MRE) [30].

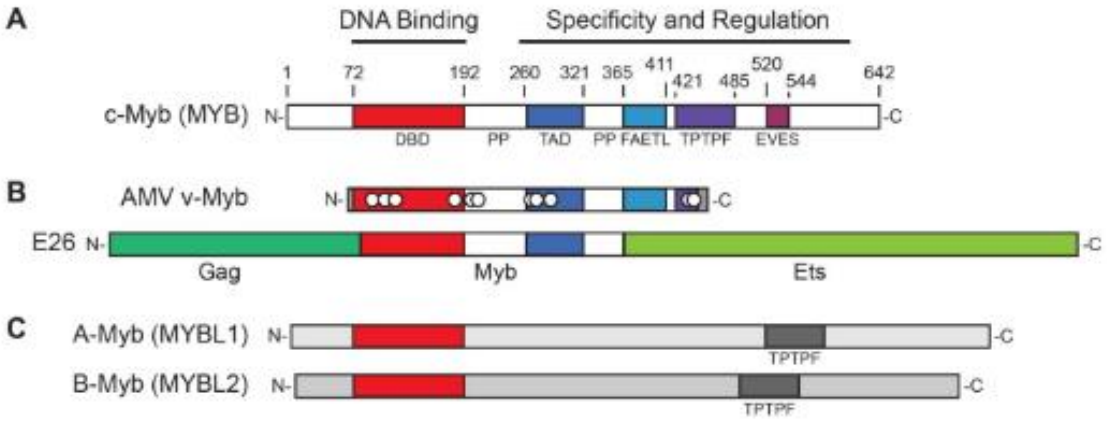

Figure 2: **Myb Protein Structures and Conserved Domains** adopted from George, O. & Ness, S. [6]

Binding to MRE was intensively studied for DBDs of functional diverse Myb related proteins. Interestingly, it was shown that observed differences between the DBDs have just minor impacts on sequence preferences within the limits of MRE [4]. Experiments with gene activity assays under the control of MRE supported this observation since they were activated by all known Myb like proteins. Based on that it was concluded that the functional diversity of Myb like proteins must be caused by other domains than the DBD or additional functions of DBD beside DNA binding [28].

Indeed, additional less conserved domains were described for gene products of the MYB family [8]. Figure 2 shows a comparison of the domain structure of c-Myb, v-Myb, A-Myb and B-Myb. The DBD (red) can be found across all Myb like proteins, because it is the defining feature. Generally, three conserved regions were identified for orthologs of c-Myb. Namely an N-terminal DBD that was previously discussed, a minimal transactivation domain (TAD) that is essential for c- Myb´ s function and a C-terminal negative regulatory region that controls the activity of c-Myb and prevents oncogenicity [5,6].

A comparison of c-Myb (A) and v-Myb (B) reveals truncations at the N and C terminus and several point mutations of v-Myb. However, the TAD and FAETL domains are present in both proteins. The function of TAD is essential for the formation of core interaction which are crucial for Myb mediated activation of gene expression. The role of the FAETL domain is less studied but mutational analysis showed that it is required for the oncogenic activity of v-Myb [6].

In contrast, A-Myb and B-Myb show a less conserved domain structure in comparison with c-Myb. The poorly investigated TPTPF domain, which can be found in the putative C-terminal negative regulatory region, is the only common feature, beside the DBD [6].

The involvement of c-Myb in cancer formation

First line of evidence that c-Myb is potentially involved in oncogenicity was provided by the close relation of c-Myb and the oncogenic v-Myb protein [8,31]. Based on that, initial research focused on c-Myb´s role in the hematopoietic systems. Indeed, knock out experiments in mice have suggested that c-Myb is essential for the development of the hematopoietic system since it regulates proliferation and differentiation of progenitor cells [4]. In line with these results it was later shown that c-Myb is often amplified or upregulated in hematopoietic malignancies with increased numbers of progenitor cells [4,5].

Recently, extensive characterization of various cancer types confirmed initial results seen for the hematopoietic malignancies and revealed that c-Myb is also involved in a large number of solid tumors, including prostate cancer [32]. Transcriptional profiling provided thereby striking insights into the involvement of c-Myb´ s c-terminal regulatory domain on oncogenesis. First, it was revealed that extensive alternative RNA splicing of several alternative exons led to great diverse of MYB genes transcripts in leukemias. Most observed alternative transcripts contained the DBD and TAD domains but showed a variety of truncations or alterations at C terminal domains, which led to a v-Myb like domain structure. Secondly, recurrent Myb-NFIB fusion transcripts were described as potential driver of Adenoid cystic carcinoma, a salivary gland tumor [6]. Strikingly, fusion transcripts contain a truncated part of Myb that reflect the domain structure of observed alternative transcripts in leukemias [6]. Because of this reoccurring pattern of C terminal truncations, it was suggested that the lack of a

functional the C -terminal negative regulatory domain might be crucial for the oncogenic potential of c-Myb [33].

At this point c-Myb´s dual role of activating proliferation and activating differentiation has to be mentioned. Although the majority of studies describe c-Myb as oncogenic driver, due to it´s potential to induce proliferation, it was also shown that c-Myb might counteract oncogenicity by inducing differentiation. Thus, highlighting the complexity of c-Myb´s function depending on the cellular environment [4].

The regulation of c-Myb

The effect of c-Myb on transcriptional programs is exceptional diverse depending on the specific cellular context [6,34]. To explain this diversity a model was suggested were c-Myb´s function is mainly dependent on protein-protein interaction to cofactors. Consequently, the cellular environment would control which complexes are formed by providing specific cofactors or by direct modulation of protein-protein interactions (PPI)[6]. The regulation of PPIs would be thereby most likely accomplished by posttranslational modifications of c-Myb or its cofactors. In line with this suggested model it was discovered that c-Myb can be subject to different post translational modification and that it can interact with a variety of cofactor including the CREB-binding protein (CBP), p300 and the TFIID subunit TAF12 [12,35].

The interaction of c-Myb and the KIX domain

The CREB-binding protein (CBP) and p300 are two closely related transcriptional co-activators that are important for transcriptional regulation. CBP and p300 possess a histone acetyltransferase (HAT) activity which enables them to change chromatin activity by epigenetic modification. In addition, CBP/p300 can influence gene expression by acting as protein bridges or scaffolds connecting the general transcriptional machinery and specific TFs like c-Myb. To facilitate this function CBP and p300 contain a conserved KIX domain that is involved in a variety of PPIs [36–38]. Extensive research was performed and revealed the importance of the interactions between the KIX domain of CPB/ p300 and the TAD of c-Myb [35]. Interestingly, it was shown that the introduction of the point mutation M303V in the c-Myb peptide disrupts the interaction with KIX and led to almost complete loss of c-Myb induced transcription [34]. Moreover, a crystal structure of the TAD of c-Myb and KIX was solved and enabled the development of an effective peptidomimetic [39]. Blockage of the interaction utilizing the peptidomimetic led to downregulation of Myb depended genes and finally cancer cell death. Based on these striking results it was suggested that a small molecule probe which blocks the interaction of c-Myb and KIX could be a potential therapeutic [39].

The interaction of c-Myb and TAF12

More recently, Chris Vakoc´s research group applied a reverse approach and revealed another crucial PPI of c-Myb that could be potentially utilized against cancer [12]. Initially the study investigated the potential of targeting specific subunit of general TFs. It was known that TFIID consists of a multitude of subunits, which vary depending on the cell type. Based on that it was proposed that pleiotropic effects of targeting general TFs could be mitigated if differential dependencies could be found for specific subunits. Indeed, TAF12 which is a critical subunit of TFIID and the SAGA complex, was discovered as a selective dependency of AML cells [10]. This dependency was traced back to c-Myb, since knock down experiments of both genes showed very similar expression patterns. Extensive research was performed and revealed TAF12 and TAD of c-Myb physically interact. Based on these results a model with potential therapeutic approach was developed and is shown in figure 3 [12].

Briefly, the interaction of c-Myb and TAF12 is important for the function and protein stability of c -Myb. TAF12 is known to form a histone fold handshake interaction with TAF4, a significantly larger subunit of TFIID. Based on that a squelching approach was developed were expression of the histone fold domain (HFD) of TAF4 is used to prevent the functional formation of c-Myb : TFIID interaction. Consequently, TAF12 can still bind to c-Myb and the HDF of TAF4 but would not interact with TFIID anymore. Application of this approach to in vitro and in vivo AML models led to potent anti-cancer effect, including extended survival of the in vivo model. Thus, it was concluded that the interaction between c-Myb and TFIID *via* TAF12 presents an interesting target for chemical probe development [12].

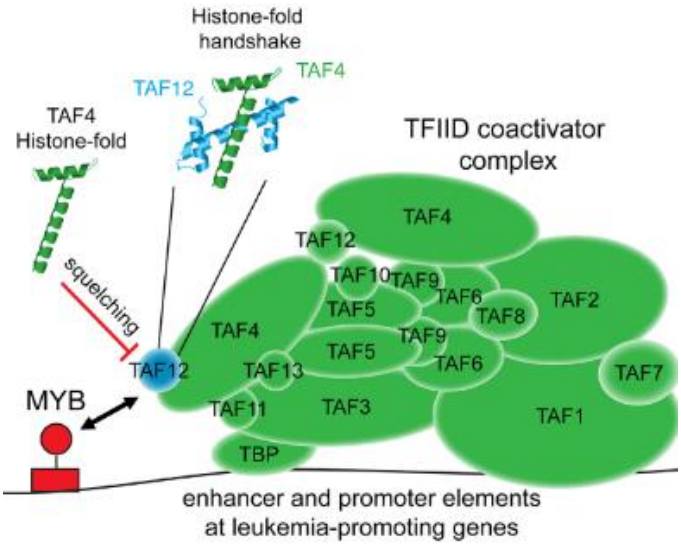

Figure 3: **Targeting the interaction of c-Myb and TFIID**, Squelching of TAF12 with a TAF4 HFD Peptide; adopted from Xu, Y., *et al*. [12]

Summarized, c-Myb is a highly complex TF that has essential functions in the development of the human body and is involved in oncogenesis. Understanding the molecular complexity of c-Myb´s

regulation remains an intriguing question. However, the discovery of two key PPIs which are crucial for c-Myb´s function provided hints how c-Myb could potentially regulate gene expression. Thus, developing high quality small molecule probes against these PPIs would be a great tool to test c-Myb´s therapeutic potential and to get more insights about its biology.

The development of small molecule probes against transcription factors

Opportunities

The potential of utilizing TFs as drug targets was hypothesized almost two decades ago when the molecular mechanisms of single TFs were deciphered [14,22,40]. Although research at that time was far away from understanding the complexity of TFs, it was strikingly enough to see the far-reaching effects of single TFs. Spectacular developments in the field of RNA sequencing enabled transcriptional profiling of a variety of cancer types and strongly supported the initial observations. Unbiased comparison of transcriptional programs of healthy and diseased tissues revealed that a high number, if not all, cancer types are driven by misregulated transcriptional programs [10,22]. Although the molecular mechanism which led to misregulation can be multifarious and is still not totally understood, it was shown that the uniting feature is altered transcription of one or many genes.

The potential of TFs as drug targets was finally confirmed by genomic dependency mapping [10]. Applying RNAi or CRISPR screenings revealed that many specific TFs are strong differential dependencies. Concise, differential dependencies are found by comparing the lethality of a knock down or knock out of a specific gene in many cell lines. Therefore, RNAi or CRISPR loss of function screenings are performed using libraries that target each individual gene of a cell. After the knockout of statically one gene per cell, high throughput sequencing of surviving cells is used to analyze the effects of each knock out. Application of complex algorithms to analyze the sequencing data showed which genes are essential depending on the cellular context. Such dependency maps revealed a number of so called common essential genes and differential dependencies which are not important for the survival of most cell lines but are essential in specific cancer cell lines [10]. Such differential dependencies present great potential for drug development because the likelihood that a therapeutic window exists for this gene is very high. Since, many specific TFs are classified as differential dependencies it became clear that it would be potentially very efficient and specific to target individual TFs [41] .

More evidence that targeting TFs could lead to very specific effects is provided by their position in signaling cascades [22]. Compared with conventional anti-cancer targets, like cell surface receptors, specific TFs are further downstream in signaling cascades. Thus, targeting TFs could be a more direct approach that tackles the root of misregulation and avoids the complexity of upstream signaling nodes. In addition to increased specificity, targeting TFs could be potentially less prone to the development

of resistances. Cancer cells commonly evolve and develop resistances against currently used targeted therapies. Thereby, the functions of an inhibited target can be restored by utilizing parallel signal cascades. In the case of target TFs directly, it is unlikely that a cell could restore a whole transcriptional program by using other signaling networks [22].

Challenges

The potential of targeting individual TFs was fortified by recent developments, but it is generally known for years. Nevertheless, almost no TF targeting drugs are available for clinical use. This raises the question how it is possible that such a potential is not used. Summarized, it is extremely challenging to find and develop drugs that target TFs. Until recent years TFs were even classified as undruggable targets since conventional drug development approaches failed broadly [15,40,42].

These challenges arise mainly due to the molecular mechanism how TFs regulate transcription. In many cases protein-protein interactions play a key role, as explained previously. This means that TFs often lack enzymatic functions, with the exception of chromatin remodelers [43]. In addition, TFs have generally a flat surface that presents a shortage of conventional binding pockets. Both reasons made it very difficult to find or rationally design small molecules that inhibit the function of TFs. Conventional approaches and techniques like high throughput enzyme activity assays, ligand mimicking or mechanism-based inhibition were simply not applicable.

Furthermore, TFs often contain intrinsically disordered regions (IDR) in their activation domains. These IDRs form stable secondary structures if bound to their interaction partners, whereas they are disordered in artificially settings or purified states. This makes it even more challenging to find druggable areas for TFs [44]. Early successes of chemical probe development targeted the most structured area of TFs, the DNA binding domain. However, due to the positive charges which is common for DNA binding domains it remains very difficult to convert such DBD binding molecules into drugs [45].

Consequential of the described reasons it remains extremely challenging to design meaningful high throughput screenings that keep the TF in native settings. The development of so-called small molecule microarrays by Angela Koehler and coworkers provides thereby an important advancement that addresses these challenges [46].

Small molecule microarray screenings

General principal

A Small molecule microarray (SMM) screening is a powerful high throughput binding assay that can be applied for chemical probe development against so far not traceable targets [46,47]. It relies on binding of the target protein to functionalized glass slides with arrayed compound libraries, as schematically depicted in figure 4 [48]. Concise, functionalized glass slides are incubated with the purified protein of interest or unpurified lysates that contain the protein of interest [47]. Subsequent, glass slides are thoroughly washed, and antibody-based detection is used to visualize bound target protein on the glass slide. Statistical analysis of the signal intensities of specific spots on the slide, which correlate to a specific small molecule, is than used to nomination putative small molecule binder [46].

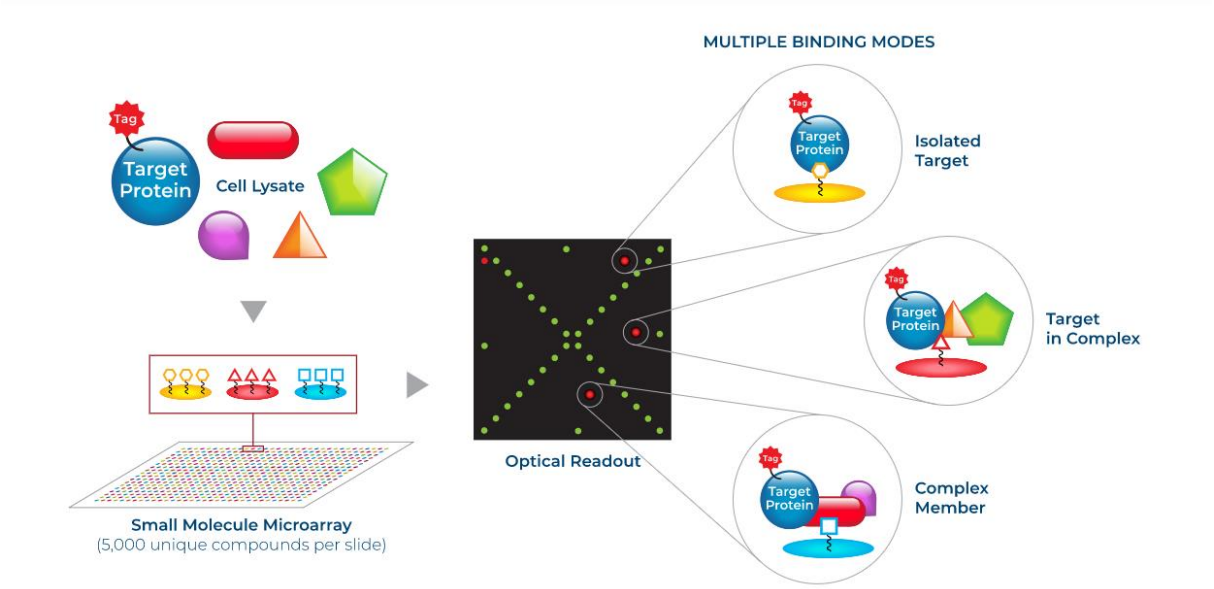

Figure 4: **The principal of small molecule microarray** adopted from Kronos Bio [48]

Incubation with target protein

SMM screenings are often applicable for challenging target protein like TFs since they allow very versatile screening conditions. The protein of interest can be screened as purified protein, in purified complexes, as in-vitro transcribed proteins or as whole cell lysate [47]. Depending on the type of screening different binding modes of the target protein and the small molecule are possible. Figure 4 depicts the most complex screening type, whole cell lysate. In such screenings target protein-small molecule interactions would be presumably detected for three distinct cases. The target protein could bind isolated to the small molecule, as it would be the case in pure protein screenings. Furthermore, the small molecule could bind at interfaces of the protein of interest and cofactors or it could bind a nearest neighbor of the target protein. Depending on the selection of downstream assays it could be

very beneficial to probe the whole network around the protein of interest. An impressive example of such a chemical probe was recently published for the interaction of Myc and Max [49].

The importance of downstream assays

SMM screenings are a high throughput technique that can be cost efficiently applied to screen then thousands of compounds. However, it is crucial to validate the hit list by secondary and most of the times also tertiary assay. The screening itself can provide a versatile technique for a variety of targets. In contrast, downstream analysis has to be thoroughly adapted for each target protein. The designing of downstream assay has to consider that SMM screenings are binding assays which does not provide information regarding the compound effect on the protein activity. This means that a variety of secondary and tertiary assays, depending on the purpose of the screening, are feasible. For the specific case of TF screening high throughput gene reporter assays, target engagement assays or protein-protein interaction assays are typically used.

Myb focused SMM screenings and the discovery of MB1 and TM1

The goal to develop high quality small molecule probe against c-Myb and related fusion proteins by deploying the steadily improving SMM platform was set by Angela Koehler's research group several years ago. In order to initiate chemical probe development against a new target, a critical path must be designed and optimized for the specific target. For the case of c-Myb, a notoriously difficult protein to work with, several challenges emerged during the development of the critical path. Although, the SMM platform is comparable flexible in terms of input material, conventional approaches to produce tagged c-Myb failed broadly due to its instability. Even lysate-based screenings of cellular overexpression systems that showed good results for other TFs were not applicable since c-Myb was rapidly degraded (unpublished results: Leifer, B.). A solution was found in a cell-free in vitro transcription and translation (IVT) method. This method is based on a cell-free HeLa derived system of enzymes and cofactors that are essential for transcription and translation. The team successfully adopted the IVT method and produced c-Myb and the fusion gene product MYB-NFIB in a good yield for the SMM platform. Most likely this method was advantageous since cellular pathways which are not active in these cell-free systems, degraded c-Myb in conventional overexpression system (unpublished results: Leifer, B.). However, it is noteworthy that these IVT systems are cell derived and that the target protein was not purified after the expression. This led to the conclusion that the presence of cofactors in the applied protein solution was more similar to a lysate screening of conventional overexpression systems than a purified protein screening. Depending on the presence of cofactors different binding modes on the SMM slide are likely, as discussed previously.

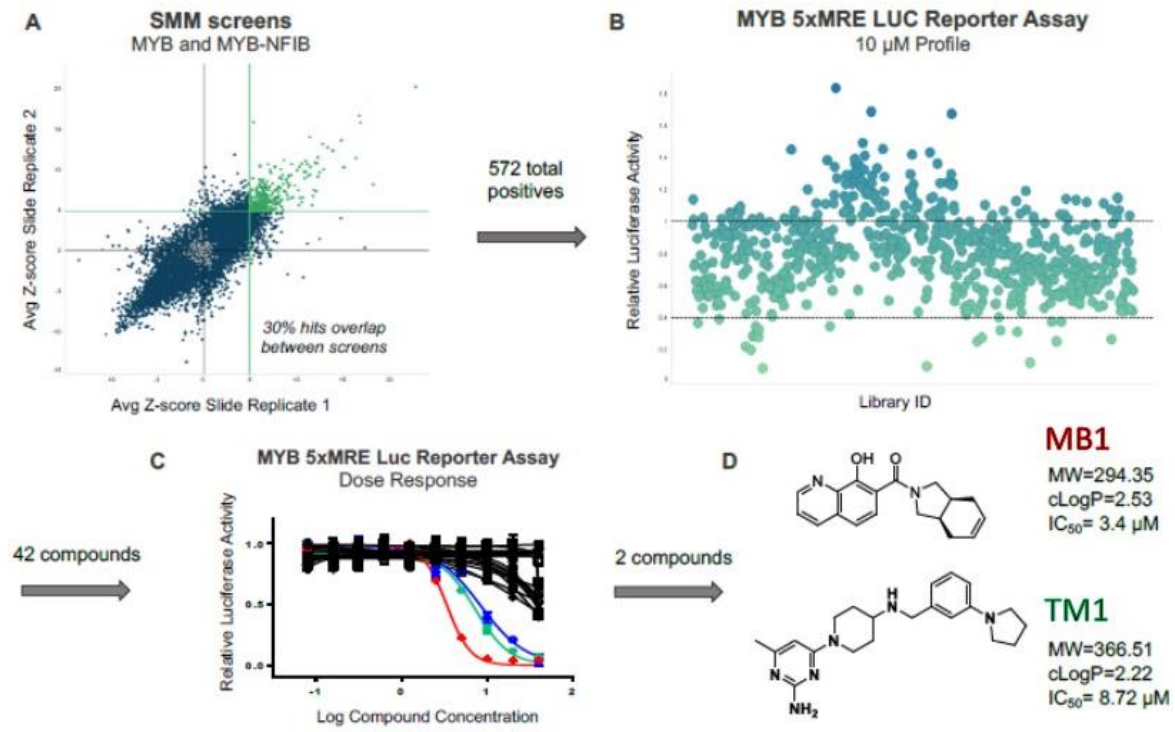

Figure 5: **The discovery of MB1 and TM1** adopted from unpublished results Leifer, B.

Figure 5 depicts the successfully applied critical path that led to the discovery of MB1 and TM1. SMM slides were printed utilizing the in-house library of the Koch Institute for Cancer research at MIT. In total approximately 50 000 small molecules were printed and screened in independent duplicates. Identification of putative hits in the SMM screens was determined by signal-to-noise ratio analysis for the fluorescence signal of each printed feature. This process provided a list of 572 compounds which were promoted to a 5xMyb-response element (MRE) luciferase reporter assays to test their potential effects on c-Myb activity. 3 compounds led to a dose dependent decrease of 5xMRE activity with IC50 values below 10µM. Based on the results of kinase inhibition profiling and histone deacetylase inhibition testing, one compound was excluded due to non-selective effect. MB1 and TM1 emerged from the critical path and were prioritized for further development (unpublished results: Leifer, B.). Figure 5 depicts the structure, chemical properties and the IC50 in the 5xMRE luciferase reporter assay of both compounds.

Results

Assay choice for the downstream analysis of SMM hit compounds

The project was initiated with the broad sub aim to advance chemical probe discovery against the TF c-Myb. To address this aim, a suitable assay had to be found for the downstream analysis of the existing hit lists. Requirements included that the assay had to be applicable for the notoriously difficult to handle c-Myb protein and that hundreds of compounds could be potentially tested. In addition, it was intended to deconvolution c-Myb´s complex biology by the application of a simplified assay setups which investigate a specific aspect of c-Myb. This was especially important since 5xMRE reporter gene assays, which were used as secondary assay, were comparably well-suited as initial filters but they had two major drawbacks. First, such assays rely on very complex biology because the activity of the tested TF could be influenced by a myriad of pathways. Second, small molecule binders that are not influencing the activity of the TF in the artificial assays system but still bind to the TF, would be missed. Biochemical assay that are performed with purified proteins can be great tool to simplify the readout. However, considering the challenges that arise during the SMM screening development it was concluded that such methods which require purified protein were not applicable. Concise, a balance had to be found to simplify the assay but keep c-Myb in physiological relevant conditions.

A potentially well-suited assay was found in bioluminescence resonance energy transfer (BRET) assays. Beside other applications, BRET assays are very useful to study PPIs between known interaction partners. The readout of BRET assays is directly dependent on an energy transfer that occurs only if the studied interaction partners are in close proximity. Thus, providing a powerful tool to screen for small molecules that block the specific PPI. Based on the literature described potential to target c-Myb´s interaction partners the idea emerged to develop and apply BRET assays for c-Myb : KIX and c-Myb : TAF12.

BRET assay development

BRET assay principal

BRET assays are live cell-based assays that rely on Förster resonance energy transfer between a bioluminescent energy donor and a fluorescent energy acceptor. [50]. BRET signals can be measured if the energy donor andthe energy acceptor are within a range of less than 10 nm [51]. Thus applying this principle for the investigation of a PPI, donor and acceptor are each fused to one of the two interaction partners of the PPI. If the proteins interact, bioluminescent energy which is generated by the fused oxidative luciferase of interaction partner 1, is transferred to the fused fluorescent acceptor of interaction partner 2 and emits the long wave BRET signal.

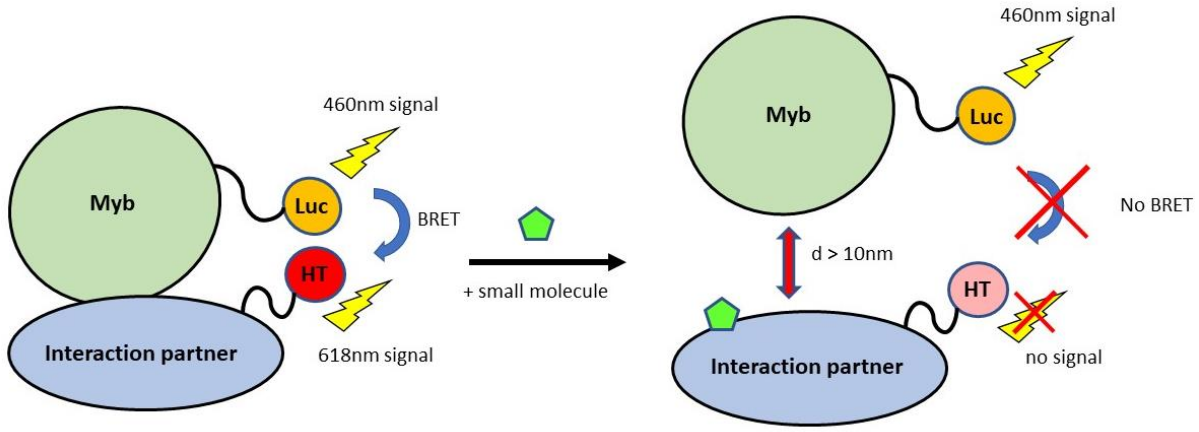

Figure 6: **Schematic representation of a Bioluminescence Resonance Energy Transfer (BRET) assay for Myb and it´s interaction partners** (e.g. TAF12), Luc: luciferase, HT: HaloTag, adopted from Powell, C., *et al.* [52]

Different BRET pairs consisting of luciferases and fluorescent proteins were developed during the last decade. [52]. The latest improvement is an engineered luciferase called NanoLuc and a long-wavelength fluorophore for the self-labelling protein tag called HaloTag. This pair is commercialized by Promega and promises higher sensitivity due to an increased spectral resolution of donor signal and acceptor signal. NanoLuc led to an improvement because it is brighter and smaller than natural luciferase. The HaloTag was chosen due to an increased wavelength of the emission signal, compared to fluorescent protein. [53].

Developing a BRET assay for a specific PPI requires the expression of fusion proteins of both interaction partners. Therefore, expression constructs of the energy donor fused to one interaction partner and the energy acceptor fused to the other interaction partner have to be designed. Fused tags could significantly influence the interaction, depending on the spatial arrangement of the PPI, the structure of the interaction partners and the orientation of fusion protein. Due to a lack of structural information for full length c-Myb and c-Myb : TAF12, all potential orientations of fusions and combinations had to be considered.

BRET assays readout and calculation

BRET assays rely on the energy transfer between a bioluminescent energy donor and a fluorescent energy acceptor, as described. Figure 7a depicts an idealized spectral representation of the NanoLuc donor signal and the Halo Ligand acceptor signal. Two different filters, shown as shaded fields, were applied to separate the donor signal and acceptor signal. The longwave acceptor signal (orange box) of a developed BRET assay is directly dependent on the energy transfer and on the donor signal. Thus, no external source of energy is used for the excitement of the acceptor, the ratio of measured acceptor signal and donor signal can be directly calculated. This ratio is the BRET readout which is internally normalized and in correlation with the investigated PPI. Thus, if a small molecule inhibits the PPI the

BRET ratio will decrease due to impeded energy transfer. Interestingly, compound mediated cytotoxicity or degradation of the donor, BRET ratios would not be reduced because of the internal normalization. This is a big advantage of BRET assays that was crucial for this study, retrospectively.

A

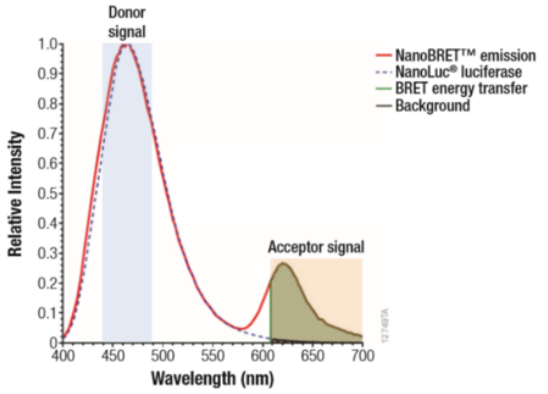

B

$$\text{mBU} = 1000 * \frac{Acceptor\ signal\ (618nm)}{Donor\ signal\ (460nm)}$$

Figure 7: **The detection and analysis of BRET assay:** a) Spectral separation of the NanoLuc® emission (460 nm) and the fluorescent HaloTag® NanoBRET™ ligand emission (618 nm b) MilliBRET ratio (mBU) calculation; both adopted from Powell, C., *et al.* [52]

Critical consideration for the development of c-Myb : KIX and c-Myb : TAF12 BRET assays

Development of the BRET assay for c-Myb : KIX and c-Myb : TAF12 started with the investigation which domains of the interaction partners are crucial for the formation of the PPI and should be therefore used for the assay. Because of c-Myb´s complex regulation and it´s intrinsically disordered regions it was concluded that full length c-Myb might be essential for a meaningful BRET assay. In the case of c-Myb´s interaction partners CBP/ p300 a crystal structure was available that showed the interaction between the TAD of c-Myb and the KIX domain of CBP/ p300. Based on that information and the sequence difference between CBP and p300 it was decided to utilize the conserved KIX domain for the BRET assay.

In contrast to the well-studied interaction c-Myb : KIX, no structural information was available for the recently discovered interaction c-Myb : TAF12. Because of that, the development of the BRET assay had to be based on co-immunoprecipitation (CoIP) studies which provided some insights into the PPI. Studies suggested that the TAD of c-Myb is essential for the interaction of c-Myb : TAF12 and that the HFD of TAF12 forms a histone fold handshake like interaction with other HFD proteins, like TAF4. Interestingly, it was shown that the overexpression of TAF12 in HEK293 cells was not possible without TAF4, suggesting that the interaction partner might be required for TAF12 stability. However, it was unclear if TAF12 and c-Myb can form a direct PPI without the presence of TAF4. Based on that limited knowledge it was decided to use full length TAF12 and a potential co-expression of the HFD of TAF4 if required, to develop the BRET assay.

BRET assay construct generation

With the aim to test all potential orientations of fusion proteins 12 BRET assay constructs had to be developed. All required BRET constructs were successfully cloned by the application of Flexicloning® (Promega). This system is based on two different antibiotic resistance and a suicide gene and offered a comparably rapid method to create various BRET constructs. The co-expression construct of the HFD of TAF4 was successfully created applying traditional restriction and ligation based molecular cloning. Expression cassettes of cloned plasmids were sequenced to ensure that the expression products were similar to the parent proteins. Table 1 shows a list of all successfully cloned and sequence verified constructs with annotated features.

Interaction partner	Fusion protein	Sequence verified
c-Myb	C-Luc	✓
	N-Luc	✓
	C-Halo	✓
	N-Halo	✓
KIX domain	C-Luc	✓
	N-Luc	✓
	C-Halo	✓
	N-Halo	✓
TAF12	C-Luc	✓
	N-Luc	✓
	C-Halo	✓
	N-Halo	✓
TAF4 HFD	Co-expression construct	✓

Table 1: Cloning of BRET expression constructs

Testing of BRET assay pairs

Successful generation of 12 BRET constructs enabled an initial BRET assay experiment that tested all potential combinations of fusion constructs. Figure 8 a and b depicts the BRET assay readout of c-Myb : KIX and c-Myb : TAF12 BRET assay orientation, respectively. Readout are shown as corrected milliBRET Units (mBU), which represent a normalized ratio of acceptor signal and donor signal that was calculated as described previously.

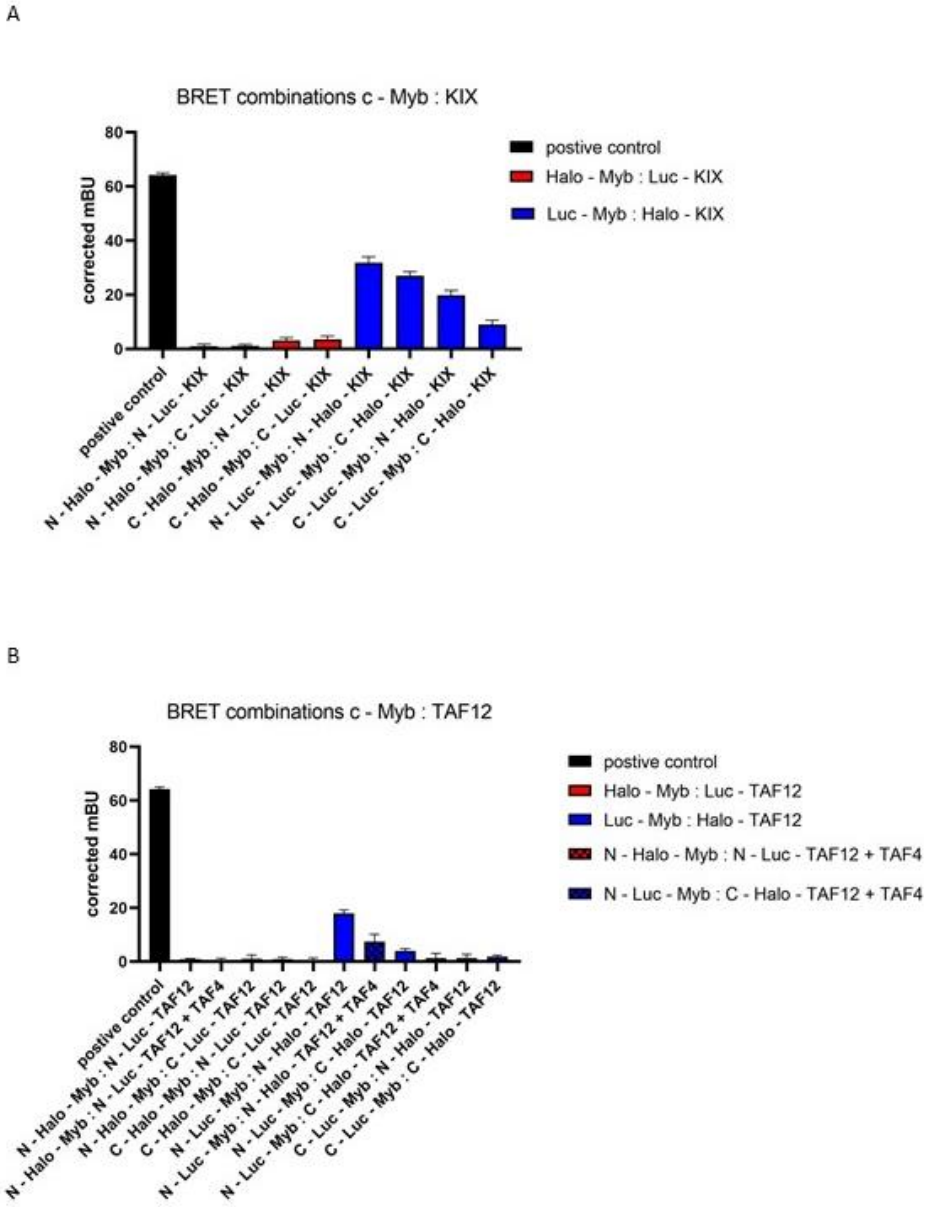

Figure 8: **Testing of BRET construct pairs**: a) Resulting BRET ratios of different fusion construct combination of c-Myb and KIX, x-axis: BRET construct combination, y-axis: calculated BRET ratios in mBU, , bars: represent the mean and the standard deviation of biological triplicates, black: positive control (p53 : Mdm2), red: Halo-Myb : Luc : KIX, blue: Luc-Myb : Halo : KIX b) Resulting BRET ratios of different fusion construct combination of c-Myb and TAF12, x-axis: BRET construct combination, y-axis: calculated BRET ratios in mBU, bars: represent the mean and the standard deviation of biological triplicates, black: positive control (p53 : Mdm2), red: Halo-Myb : Luc-TAF12, blue: Luc-Myb : Halo-TAF12, dashed bars: co-expression of TAF4 HFD

The positive control is an optimized BRET assay that was developed by the supplier for the known interaction of p53 : Mdm2. It was used as comparison to ensure a proper technical implementation and calculation. The positive control led to a corrected mBU that was greater than 60, as presented in figure 8 as black bar. Corrected mBUs of BRET assays at developmental stages are shown as red and blue bar. Red bars have in common that they represent BRET assays performed with the acceptor fused to c-Myb (Halo-Myb). Whereas blue bars have in common that they represent BRET assays performed with the donor fused to c-Myb (Luc-Myb). Labels on the x-axis are matched with table 1 and show the interaction partner, the type of the fusion protein and the terminus were the fusion occurred.

Depicted BRET ratios are directly depending on the occurrence of the energy transfer, as explained previously. Thus, the ratio of expressed donor and acceptor proteins is critical for the BRET assay and has to be matched. Concise, it is favorable that donor signals are low to prevent an overlay of the acceptor signal and that the amount of acceptor protein is high to almost saturate the PPI. Because of that, depicted mBUs are critically influenced by the rate of stably expressed donor and acceptor fusion protein and by their potential to form a PPI.

Tested combinations showed that BRET assays performed with the acceptor fused to c-Myb (red bars) yield generally very low BRET rations. In contrast, some combinations with the donor fused to c-Myb (blue bars) led to very promising results.

In the case of c-Myb : KIX (Figure 8a) NanoLuc fused to the N terminus of c-Myb combined with HaloTag fused the N terminus of the KIX domain gave the highest mBU. Combinations were the C terminus of the interaction partner was used for the fusion demonstrated lower mBUs. Interestingly, if both interaction partners were tagged at its C terminus BRET ratios decreased further which suggested a combinatorial mechanism.

In the case of the c-Myb : TAF12 (Figure 8b) BRET development, fusion construct combinations revealed a comparable behavior. NanoLuc fused to the N terminus of c-Myb combined with HaloTag fused to the N terminus of the TAF12 domain gave the highest mBU. All other combinations yield very low BRET ratios. In addition, the co-expression of TAF4 was tested and is presented in Figure 8b as black doted bar next to corresponding condition without TAF4. Short, co-expression of the HFD of TAF4 did not affect the BRET assay positively.

Additional to the depicted BRET ratios, measured donor signals were utilized as informative readout of the initial BRET experiment. The mean of measured luminescence was thereby used as a proximation of the amount of present donor fusion protein. The results suggested that high amounts of stable NanoLuc-KIX were present in the assay cells. NanoLuc-TAF12 expression appeared to be slightly less but against raised concerns co-expression of another HFD was not required for stable

expression. NanoLuc-Myb seemed to be the least stable fusion protein. Signals were high enough for stable detection but were significantly lower than TAF12 or KIX fusions. Interestingly, the signal intensity of NanoLuc-Myb samples was approximately as high as the donor signal of the developed positive control. This was in line with previously discussed considerations regarding favorable fusion protein amounts of a BRET assay and confirmed that combinations of NanoLuc-Myb in combination with tagged acceptor fusion proteins should yield the best ratios.

Summarized, this experiment revealed at least one promising BRET construct combination for each investigated PPI and enabled further development.

BRET assay optimization

Based on the findings of the initial BRET experiment promising BRET combinations were further optimized and tested. Due to the described importance of the amount of donor and acceptor fusion proteins, quantities of transfected plasmid had to be fine tuned. In addition, plasmid production was upscaled which included an extra step to remove endotoxins and handling of the assay in general was optimized to allow compound testing. Moreover, the incubation time of transfected assay cells was reduced from 24 hours to 12 hours. Figure 9 depicts the result of the optimized BRET experiment testing different amounts of donor expression construct. Corrected mBU of tested conditions (black bars) are plotted on the left y-axis. The mean acceptor signal (RFU) of each condition (red bar) was essential for the interpretation of the data and is therefore plotted on the right y-axis.

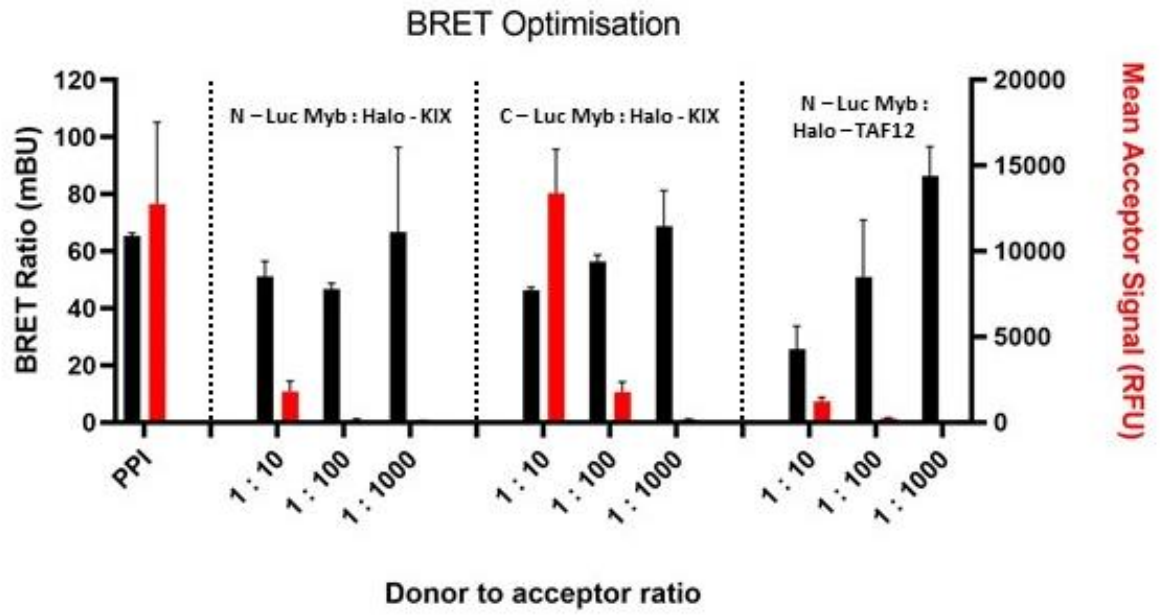

Figure 9: **Results of BRET assay optimization and donor dilution,** x-axis: donor to acceptor ratio of the quantity of used plasmids, left y-axis: calculated BRET ratios in mBU (black bars), right y-axis: mean acceptor signal in RFU (red bars), bars: represent the mean and the standard deviation of biological triplicates, bars are grouped according to utilized BRET constructs, left: positive control, two in the middle: c-Myb : KIX, right: c-Myb : TAF12

The optimized BRET assay for p53 : Mdm2 was again used as positive control. This allowed to differentiate how applied changes affected the BRET assay in general and how c-Myb focused BRET assays were affected. Interestingly, the positive control remained stable with a mean corrected mBU of 65 for applied optimizations and 64 before changes were performed. In contrast, c-Myb focused BRET assays that were performed with the same donor and acceptor construct amounts as in the previous BRET experiment, showed a significantly increased mBU. In the case of c-Myb : KIX the mean BRET ratio increased from 31 to 46, for c-Myb : TAF12 an increase from 18 mBU to 25mBU was seen. Identified improvements suggested that the shorter incubation time and adapted plasmid production was beneficial for c-Myb focused BRET assays.

The other tested variable, donor construct quantity, was more difficult to interpret. Two promising BRET assays for c-Myb : KIX and one for c-Myb : TAF12 were tested with three different donor to acceptor plasmid ratios. Therefore, the amount of acceptor construct was kept stable and the amount of donor construct was decreased to match a 1:10, 1:100 and 1:1000 donor to acceptor plasmid ratio. The aim of this experiment was to investigate if a decreased donor signal would lead to an increased BRET ratio, which would provide a favorable assay window. Indeed, a slightly increased BRET ratio and almost a two-fold increase was observed for KIX and TAF12 focused BRET assays, respectively. However, it was also observed that the stability of the assay decreased significantly with lower donor signals, which correlates with increasing error bars. Direct comparison of the positive control pair including MDM2 in a 1:100 ratio with the c-Myb assay set ups in a 1:10 ratio pointed out the generally lower signal received for the c-Myb pairs. A further decrease of the acceptor signal which was the logical consequence of a lower quantity of donor plasmid led to acceptor signals that were near the limit of detection. Thus, it was decided to continue with a 1:10 ratio and to build on the sufficiently high and stable BRET ratios which were achieved by the applied optimizations.

The lack of well described compounds that disrupt the investigated interactions prevented the implementation of further test experiments. Due to the biophysical principal of BRET assays and the way how mBU is calculated, readouts from the assay itself were used to confirm that the acceptor signal is directly dependent on the energy transfer. Therefore, a no Halo-Ligand control was utilized which contained the donor and acceptor proteins but lacks the for the energy transfer critical fluorophore. Such a control was measured for each BRET assay and was used to correct for background signal and the bleed through of donor signal into the acceptor channel. Thus, reported BRET ratios reflect the increase in acceptor signal that was observed after the addition of the critical fluorophore. Based on the results which are shown in Figure 8, it was concluded that the observed BRET ratios are directly dependent on the PPI.

Concise, we were able to develop, optimize and confirm BRET assays for the PPI of c-Myb : KIX and for c-Myb : TAF12. Both assays showed acceptable assay windows and good stability. Building on this achievement, BRET assays were applied to find small molecule probes that affect the investigated interactions.

The application of established BRET assays

With the aim to find small molecules probes that affect c-Myb´s interactome or c-Myb itself both developed BRET assays were used for testing. Experiments started with the two most promising SMM hit that led to a dose dependent decrease in c-Myb activity in the reporter gene assay. Depending on the gathered results larger SMM hits lists could have followed.

The effects of TM1 and MB1 on c- Myb : TAF12

The developed BRET assay investigating c-Myb : TAF12 was performed in a dose-dependent manner for MB1 and TM1 ranging from 0.3125 µM to 40 µM. BRET ratios were calculated as described in figure 7 and curve fitting was applied. Resulting mBU curves are depicted in figure 10 as black line and red line for MB1 and TM1, respectively. Compellingly, TM1 led to a dose dependent decrease of the BRET ratio with an IC50 of approximately 7 µM. In contrast MB1 did not affect the BRET ratios in a dose dependent manner. Except a slight increase in mBU at the highest dose of MB1 no significant changes were observed. This suggested that TM1 caused reduced interaction of c- Myb and TAF12 with an unknown mechanism. Whereas MB1 did not effect the interaction significantly.

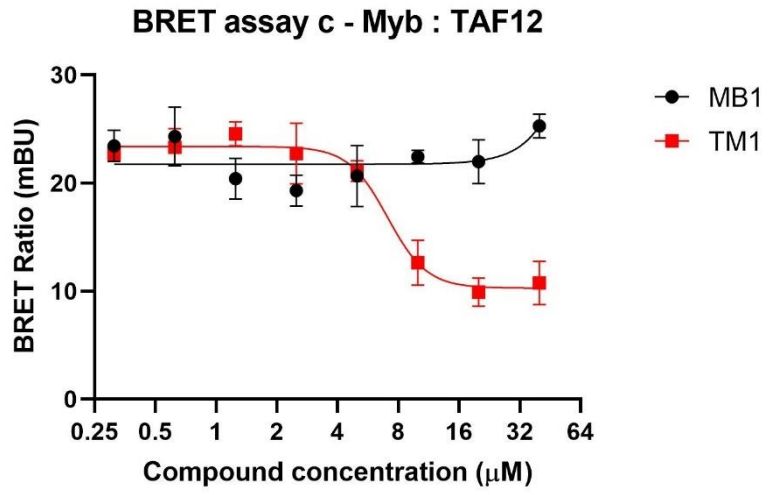

Figure 10: **The effects of MB1 and TM1 on the BRET assay c-Myb : TAF12,** dose dependent TM1 mediated inhibition of c-Myb : TAF12 with an IC50 value of approximately 7 µM, compound exposure 6h, x-axis: compounds concentration in µM, y-axis: calculated BRET ratios in mBU, data points: represent the mean and the standard deviation of biological triplicates, curves: nonlinear regression of collected data points, red: dose curve TM1, black: dose curve MB1

Provided results of the reporter gene assay were used as additional source of comparison data. TM1 inhibited the activity of c-Myb in the reporter gene assay with an IC50 of approximately 8 µM, which was strikingly similar to the calculated IC50 of the BRET assay. MB1 led to an IC50 of approximately 3.5 µM in gene reporter assay but was inactive the c-Myb : TAF12 BRET assay. The observed difference supported the reported results for TM1 and suggested that the compounds might have different mode of actions.

The effects of TM1 and its structurally related negative control on c-Myb : TAF12

To confirm the promising results of TM1 in the BRET assay for c -Myb : TAF12 additional compounds with characterized features were tested. The same BRET assay setup was utilized for those compounds to investigate if BRET ratios would change.

Gathered results raised interest in the chemical structure of TM1 and led to a fruitful collaboration with chemists of the Koehler lab. The point was raised that a critical step for every chemical probe development series is the synthesis of a structural related negative control. Thankfully, chemists were able to synthesis a derivative of TM1 that harbored minor chemical modifications but led to a significantly reduced activity in the 5xMRE reporter gene assay. A structurally related negative control of TM1 that led to an IC50 value above 40 µM in the gene activity assay, was utilized for a direct comparison with TM1. Figure 11 displays the results of the performed BRET assay comparing the effects of TM1 (red line) and the structurally related negative control (black line). In contrast to TM1, no dose dependent decrease of the BRET ratio was observed for the negative control. A slight decrease of the BRET ratio was mediated by the highest applied concentration (40 µM) of the negative control. This minor effect was also observed in the reporter gene assay and suggested weak activity of the derivative. However, the clearly distinct effects of TM1 and its structurally related negative control supported the previously reported results and suggested putative structure activity relationship of TM1.

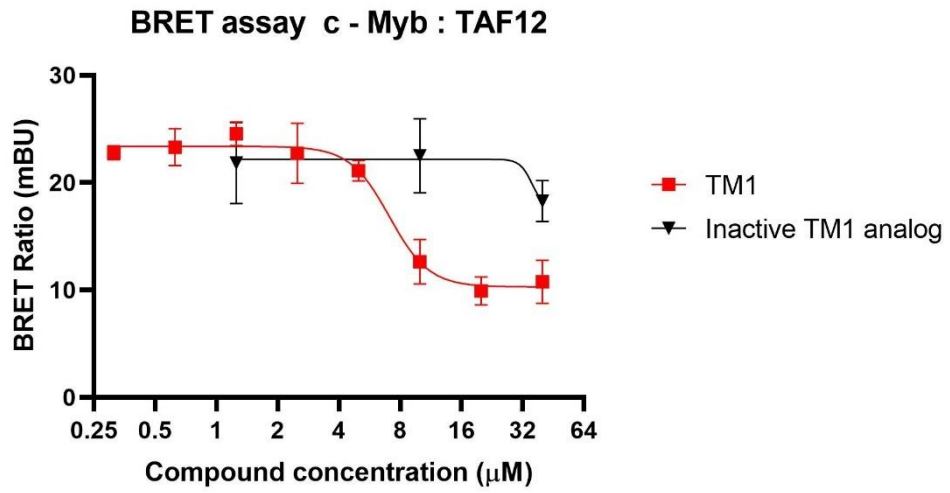

Figure 11: **The effects of TM1 and its structurally related negative control on the BRET assay c-Myb : TAF12,** dose dependent TM1 mediated inhibition of c-Myb : TAF12 with an IC50 value of approximately 7 µM, compound exposure 6h, no significant inhibition observed for its structurally related negative control, x-axis: compounds concentration in µM, y-axis: calculated BRET ratios in mBU, data points: represent the mean and the standard deviation of biological triplicates, curves: nonlinear regression of collected data points, red: dose curve TM1, black: dose curve of the structurally related negative control of TM1

Gaining more insights into the BRET ratios of c-Myb : TAF12

The TM1 mediated dose dependent decrease of the BRET ratio and the inactivity of TM1´ s structurally related negative control were intriguing. However, the lack of proper control compounds for the development of the c-Myb : TAF12 BRET assay made it challenging to compare and interpret the observed BRET ratio changes. Concerns were raised how the BRET assay would react to cytotoxic compounds or c-Myb degrading compounds. To address this question a recently discovered c-Myb degrader, named mebendazole, was utilized as comparison for TM1.

Mebendazole is a structurally unrelated repurposed anti-helminth agent that leads to proteasome dependent degradation of c-Myb. Its effect on c-Myb was recently discovery during a repurposing screening that was based on a comparison of transcriptional signatures. In vitro studies showed that a 6 hour treatment of 10 µM mebendazole led to almost complete degradation of c-Myb, presumably mediated *via* a the heatshockprotein 70 pathway. For further characterization of the c-Myb focused BRET assay mebendazole was applied as a tool compound to figure out if c-Myb degradation could be the reason for a decreased BRET ratio.

Figure 12 presents the calculated mBU of dose-dependent treatment of MB1 (black), TM1 (red) and mebendazole (blue). Surprisingly, mebendazole caused an increase of the BRET ratio that peaked at around 10 µM. This result was the opposite to raised concerns and was significantly different than the effects of MB1 and TM1. An increase of the BRET ratio could be theoretically caused by an increase of the acceptor signal due to induced interaction or by an alteration of donor and acceptor protein amounts. Based on the published effect of mebendazole to degrade c-Myb, it was concluded that the

degradation of the NanoLuc-Myb led to a comparable effect as seen for lower quantities of the donor plasmid (Figure 9). In addition to the depicted BRET ratios, mean donor signals were analyzed which pointed out that mebendazole led to dose dependent decrease of the NanoLuc-c-Myb signal. Noteworthy, a more significant decrease of the donor signal was seen for MB1. In retrospect, it was shown that MB1 can induce apoptosis within a few hours. Thus, providing a valuable comparison as immediate cytotoxic compound.

Summarized, the observed BRET ratios for a cytotoxic compound and a c-Myb degrading compound strongly supported the developed c-Myb : TAF12 BRET assay. No other compounds than TM1 did cause a significant decrease in the BRET ratio which emphasized the effect of TM1.

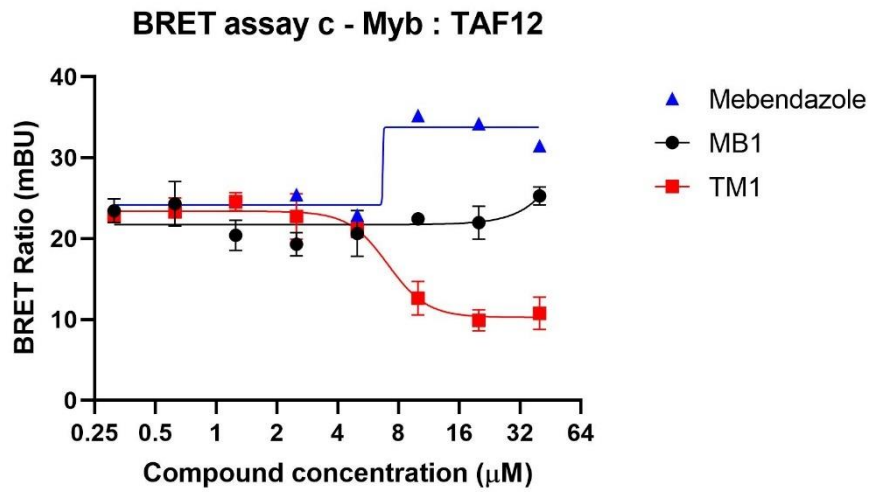

Figure 12: **The effects of TM1, MB1 and mebendazole on the BRET assay c-Myb : TAF12** dose dependent TM1 mediated inhibition of c-Myb : TAF12 with an IC50 value of approximately 7 µM, compound exposure 6h, clearly distinct effects of the c -Myb degrader mebendazole**,** x-axis: compounds concentration in µM, y-axis: calculated BRET ratios in mBU, data points: represent the mean and the standard deviation of biological triplicates, curves: nonlinear regression of collected data points, red: dose curve TM1, black: dose curve MB1, blue: dose curve mebendazole

The effects of TM1 and MB1 on c-Myb : KIX

Based on the promising results of performed BRET experiments and the encouraging insights into the effect of TM1, the second developed BRET assay focusing on c-Myb : KIX was applied. Especially in the case of TM1 it served as valuable control to answer if TM1 mediated effects were specific for c-Myb : TAF12 or not.

Figure 13 depicts the calculated BRET ratios and curve fitting for a dose curve of MB1 (black) and TM1 (red) ranging from 0.3125 µM to 40 µM. No significant changes in the calculated BRET ratios were observed for MB1 treatments. This suggested that neither c-Myb : TAF12 nor c-Myb : KIX is influenced by MB1. TM1 mediated effects on c-Myb : KIX were more complex. A weak but statistically significant and recurring decrease of the BRET ratio was observed at concentrations higher than 5 µM. Although

the shown curve fitting has to be carefully interpreted due to small effect size, it is noteworthy that an IC50 of approximately 7 µM was reported. The similarity in reported TM1 IC50 concentrations for c-Myb : TAF12 and c-Myb : KIX BRET assay and the different effect sizes were striking.

Summarized, results suggested that TM1 has a weak effect on the interaction of c-Myb : KIX with approximately the same IC50 concentration as the interaction of c-Myb : TAF12 is putatively disrupted. However, due to the complexity of c-Myb´s regulation and unresolved questions about c-Myb´s interactome further experiments were required to enable more insights regarding the mode of action of TM1.

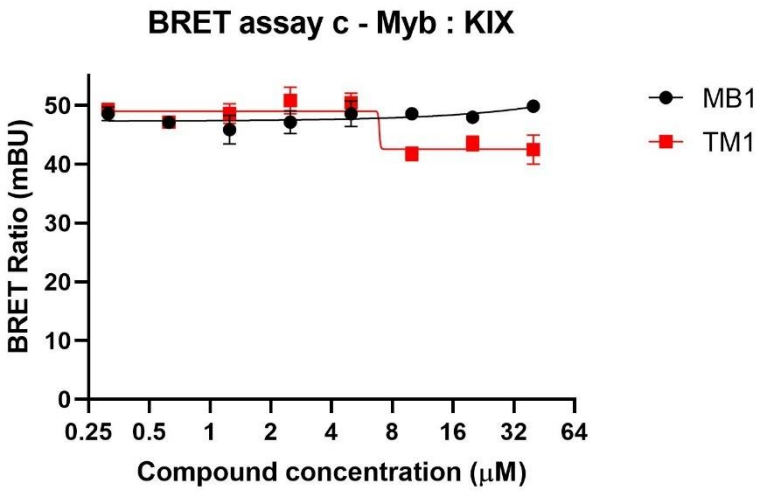

Figure 13: **The effects of MB1 and TM1 on the BRET assay c-Myb : KIX,** weak dose dependent TM1 mediated effect of c-Myb : KIX, IC50 value approximately 7 µM, compound exposure 6h, x-axis: compounds concentration in µM, y-axis: calculated BRET ratios in mBU, data points: represent the mean and the standard deviation of biological triplicates, curves: nonlinear regression of collected data points, red: dose curve TM1, black: dose curve MB1

Biological effects of MB1 and TM1

Despite the intriguing results of the BRET assays in case of TM1 and the observed inhibition of gene reporter assay for MB1 and TM1, relatively little was known about the compounds. Further characterization of biological effects was required to confirm the suggested potential and to launch a comprehensive development series. Therefore, an initial experiment was performed which investigated MB1 and TM1 mediated effects on cell viability and on c-Myb protein level. Jurkat cells, a human T lymphocyte cell line, was utilized for the endogenous gene reporter assay of c-Myb that was performed as secondary assay of the critical path. Based on that and a comparable high expression of c-Myb Jurkat cells were used as vitro model for initial testing of compound effects.

Figure 14 shows a summary of compound induced c-Myb protein level and cell viability changes, relatively to the according DMSO control. Protein level measurements were performed applying quantitative western blotting normalized against the loading control histone 3 (H3). Present ATP levels

were measured with cell titer glow (CTG) and used as a proximation of cell viability. Compound effects were investigated at a long timepoint (Figure 14a) and a short timepoint (Figure 14b). Long timepoints were treated for 24h with a low (5 µM) and high (20 µM) dose of compound. Short time points were performed with the aim to investigate more rapid effect and were therefore treated with 20 µM (high dose) of compound.

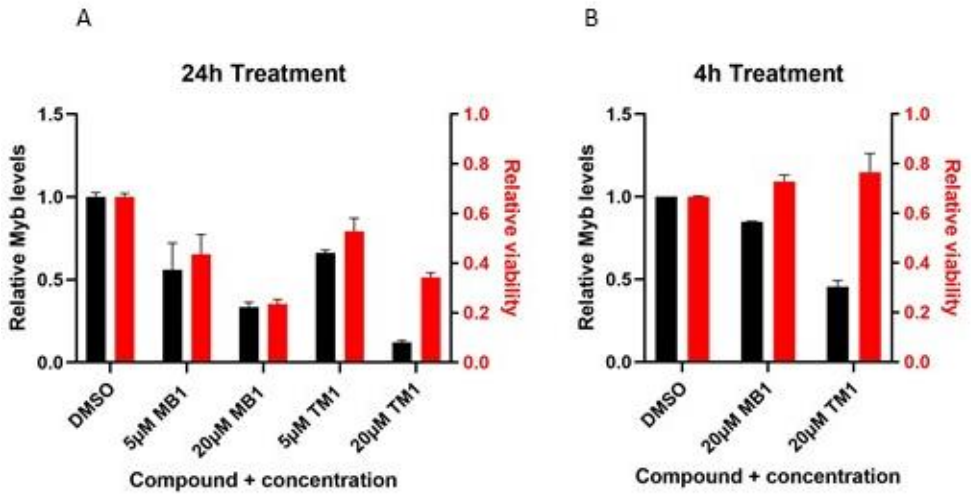

Figure 14: **The effects of MB1 and TM1 on cell viability and c-Myb protein levels,** a) Investigation of compound mediated effect on Jurkat cells that were exposed to compounds for 24h, x-axis: treatment conditions, left y-axis: relative c-Myb protein levels determined by quantitative western blotting, H3 utilized as loading control, right y-axis: relative cell viability determined by cell titer glow measurements, bars: represent the mean and the standard deviation of biological triplicates (cell viability) and duplicates (c-Myb protein quantification), b) Investigation of compound mediated effect on Jurkat cells that were exposed to compounds for 4h, procedure and labeling of the graph as described for part a

Relative cell viability after 24h compound treatment revealed that both compounds had cytotoxic effects against T lymphocytes. Encouragingly, low and high doses of both compounds led to significantly decreased cell viability of the Jurkat cells, visualized by the red bar in figure 14a. The observed reduction was comparable for both compounds and correlated with the amount of applied compound. Relative protein levels of c-Myb (black bars) were also affected by 24h compound treatments. However, due to the long incubation time it was unclear if seen changes were caused by cytotoxicity of the compounds or if c-Myb was directly affected. Nevertheless, a comparison of the relative protein levels after MB1 and TM1 treatments was interesting since significant differences were observed. Intriguingly, a 90% reduction of c-Myb was observed for 20 µM of TM1 without a more prominent viability effect than MB1.

This effect was in accordance observed results of short timepoints (Figure 14b). High dose treatments of MB1 led to a weak decrease in c-Myb level whereas TM1 reduced c-Myb levels by more than 50%. This suggested a potential direct mechanism of TM1 on the biology of c-Myb. ATP levels of treated

cells were slightly increased by both compounds after 4h exposure. However, it has to be mentioned that CTG based measurements after short timepoints have a limited explanatory power due to a lack to sense the activation of programmed cell death.

Summarized, it was revealed that both compounds have cytotoxic activity against the T lymphocyte cell line, Jurkat. In addition, significant differences in compound mediated effects were observed and suggested a distinct mode of action. In the case of TM1, a rapid compound induced reduction of c-Myb protein levels was discovered. This was especially compelling because of a potential link to interaction of c-Myb : TAF12. Published data from the Chris Vakoc´s study that investigated the interaction suggested that TAF12 is required for the stability of c-Myb. Thus, the cytotoxic effect of TM1, the induced BRET ratio decrease and the reduction of c-Myb level were highly intriguing. Based on that it was decided to prioritize TM1 and to investigate its biological effects in more details.

The effects of TM1 on c-Myb protein levels

Results of the initial experiment provided encouraging Insights into TM1´ s biological effects. Yet a detailed investigation of protein level changes was required to interpret and predict the effect of TM1.

A challenge that had to be addressed previous to further investigation was the choice of a proper in vitro model. The TF c-Myb has a short half life and is a generally low expressed protein. This made it difficult to perform precise quantitative western blotting. Handling optimization and the use of Jurkat cells, a cell lines with comparably high c-Myb expression, enabled the initial test experiment. Despite measured signals were still weak and Jurkat cells were comparably poorly profiled. A solution was found in the T lymphoblast cell line, Molt4. A comparison of published MYB RNA expression levels revealed that Molt4 had the highest mRNA levels of c-Myb (The human protein atlas [54]). In addition, Molt4 cells were well profiled and could be found in several informative data bases. Thus, Molt4 provided the optimal in vitro system to further investigate the biological effect of TM1.

With the aim to obtain an understanding of the dose dependency, time dependency and potential involvement of the proteasome, a series of experiments with varying conditions was performed.

Figure 15 presents the effects on c-Myb protein levels of a TM1 dose curve In the presence and absence of the proteasome inhibitor MG132. Protein levels were measured applying quantitative western blotting and were normalized against the according +MG132 or -MG132 DMSO control. Molt4 cells were treated for 6h with a dose curve ranging from 1.25 µM to 40 µM TM1. Co-treatment of DMSO (red line) or MG132 (black line) was performed 30 minutes previous to TM1 treatments.

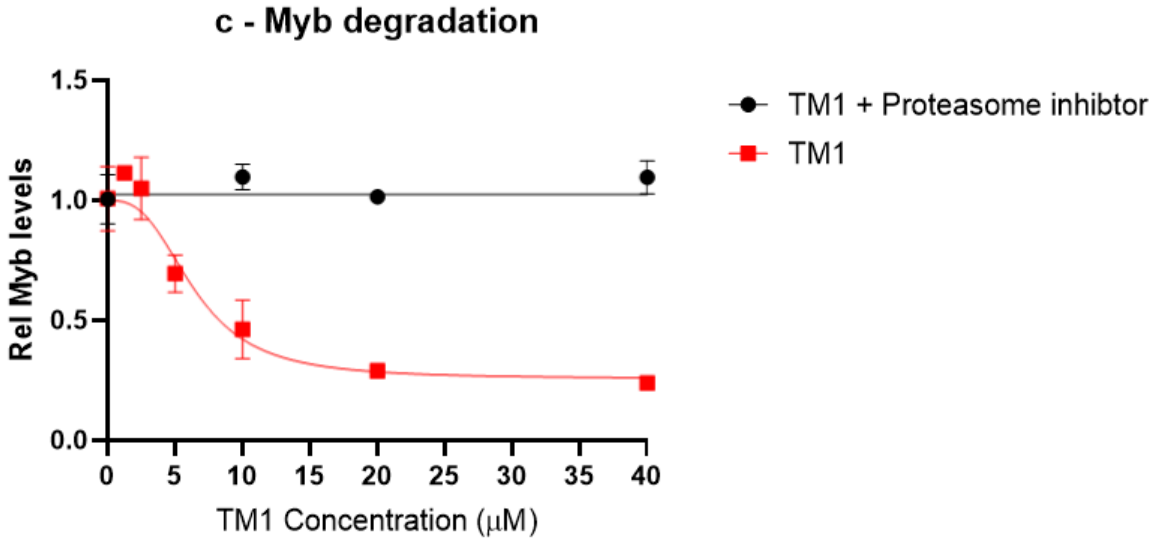

Figure 15: **The effect of TM1 on c-Myb protein levels in the absence and presence of a proteasome inhibitor,** quantification of c-Myb protein levels in Molt4 after 6h compound exposure, TM1 mediated dose dependent decrease of c -Myb levels, co-treatment of a proteasome inhibitor impeded the effect, x-axis: TM1 concentration in µM, y-axis: relative c-Myb protein levels determined by quantitative western blotting, H3 utilized as loading control, data points: represent the mean and the standard deviation of biological duplicates, curves: nonlinear regression of collected data points, red: dose curve TM1, black: dose curve TM1 + co-treatment of 10 µM MG132

In absence of the proteasome inhibitor MG132, TM1 led to a dose dependent decrease of c-Myb levels, which confirmed the results of the initial experiment. Curve fitting showed a sigmoid effect curve of TM1 with EC50 concentration of approximately 7 µM. As depicted by the red line in figure 15, a significant reduction of c-Myb started at 5 µM TM1 and saturated at 20 µM TM1. Note, that a treatment of Molt4 with 20 µM TM1 for 6h caused a c-Myb protein level reduction of more than 75%. Compellingly, co-treatments of MG132 rescued c-Myb levels completely. Even at the highest concentration of 40 µM no decrease in c-Myb protein level was observed, as depicted by the black line. The successful rescue of TM1 induced reduction of c-Myb levels with a proteasome inhibitor suggested that the reduction was proteasome dependent.

In addition to c-Myb protein levels the quantities of present TAF12 were measured for all data points. The measurement was intent based on the previously mentioned linage of TAF12 and c -Myb stability and initial result of c-Myb reduction. However, no significant changes in the TAF12 protein levels were observed after TM1 treatment with or without MG132.

With the aim to get a better understanding of the kinetics of the observed effects a time series experiment was performed. Figure 16 presents a red and black timeline of c-Myb levels after TM1 treatments of 10 µM and 20 µM, respectively. Protein level were measured every 2 hours after the treatment with 20 µM TM1. Surprisingly, c-Myb protein levels dropped during the first two hours after the treatment and were stable low until the last measured timepoint, indicated by the black dashed line. To investigate the unexpected rapid effect of TM1, the dose was decreased to 10 µM and an

additional short timepoint was collected after one-hour post treatment. The result of the 10 µM timeline are depicted as red line.

Overall, treatments of TM1 led to a fast time dependent decrease of c-Myb with varying kinetics. 10 µM treatment induced a less marked and slower reduction of c-Myb levels than the 20 µM treatment. The relative decrease of c-Myb levels after 10 µM treatment peaked during the first two hours and was significantly slower after 4 hours. The relative decrease after 20 µM treatments showed a comparable but more prominent trend. Concise, the results suggested that TM1 led to an exponential reduction of c-Myb levels. The concentration of TM1 thereby presumably defines the extend of the decrease and the shape of the curve.

Summarized, experiments which focused on TM1 induced c-Myb protein level changes in the model system of Molt4, confirmed initially observed effects and provided striking insights. It was shown that co-treatment of the proteasome inhibitor MG132 rescued the TM1 induced reduction of c-Myb completely. This suggested that the TM1 induced reduction of c-Myb is proteasome mediated. In addition, dose dependency of TM1 with an EC of approximately 5 µM was shown for the reduction of c-Myb levels. Moreover, an intriguing similarity of reported IC50s and EC50 of the BRET assay, the reporter gene assay and c-Myb level reduction was found. Furthermore, observed protein level changes suggested that TM1 induced reduction of c-Myb follows an exponential decay. Effect size and reduction rates were thereby dependent on the compound concentration with higher

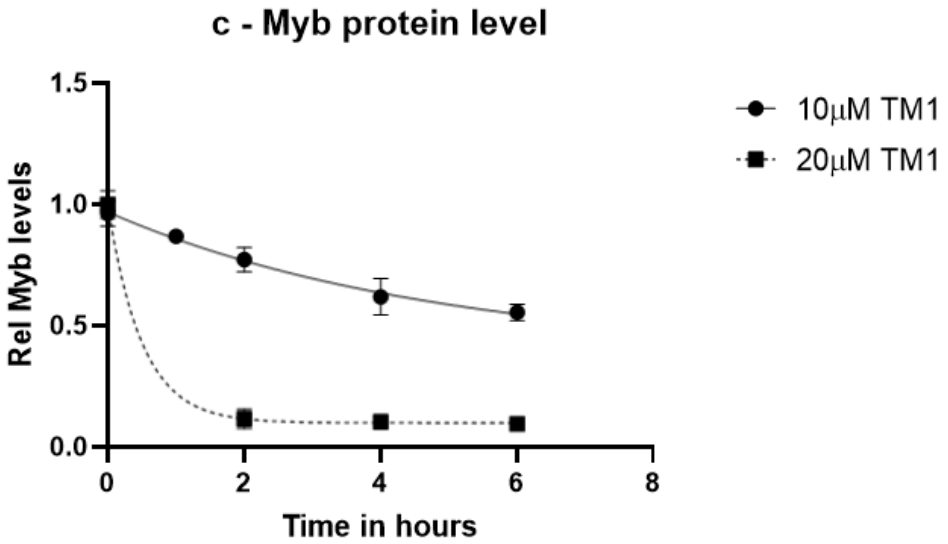

Figure 16: **The effect of TM1 on c-Myb protein levels over time,** quantification of c-Myb protein levels in Molt4 after varying times of exposure to 10 µM or 20 µM TM1, TM1 mediated exponential decay of c -Myb protein levels over time, x-axis: exposure time in hours, y-axis: relative c-Myb protein levels determined by quantitative western blotting, H3 utilized as loading control, data points: represent the mean and the standard deviation of biological duplicates, curves: nonlinear regression of collected data points, black: 10 µM TM1, dashed black: 20 µM TM1

The effects of TM1 on the relative expression of MYB and MYC

With the aim to enhance the understanding of TM1´s biological effect, transcriptional changes were examined after compound exposure. Therefore, the expression of MYB, MYC and CCNB1 normalized to the housekeeping gene GAPDH were measured via quantitative polymerase chain reaction (qPCR). Investigation of the gene expression level of MYB after TM1 treatments was critical for the interpretation of observed c-Myb protein level changes. In addition, MYC and CCNB1 gene expression was chosen due to published data that shows Myb occupancy at their promotor region and suggests a direct linkage.

To enhance the interpretability of expected results and mirror the conditions of previously performed experiments a broad range of compound concentrations and time points was tested. Therefore, the T lymphoblast cell line Molt4 was treated for 1, 2, 4, 6 and 8 hours with 5, 10 and 20 µM of TM1. In addition, a selection of conditions was co-treated with the proteasome inhibitor MG132, to reflect the protein level rescue. The treated cells were harvested and the RNA was extracted in a plate based format. Resulting RNA was transcribed into cDNA and used as input for the qPCR.

Figure 17 depicts the relative expression of MYB (left part) and MYC (right part) measured after a time series of TM1 treatments with 5, 10 and 20 µM. Bars are grouped according to the treatment condition and represent the data of biological duplicates in technical triplicates. Expression levels were calculated relative to the 8h DMSO control utilizing the 2^-ΔΔCt method. DMSO controls of each timepoint (data not shown in the graph) were collected and analyzed to asses a potential influence of DMSO and the stability of the performed experiment. Reassuringly, no significant differences were observed for the relative expression of MYB and MYC. In contrast, CCNB1, the third measured gene, was excluded from the analysis due to high variance and a lack of meaningful results. CCNB1 expression was generally lower than MYB and MYC expression which might be the reason that the assay was less stable. However, analyzed results suggested that TM1 did not influence CCNB1 expression significantly.

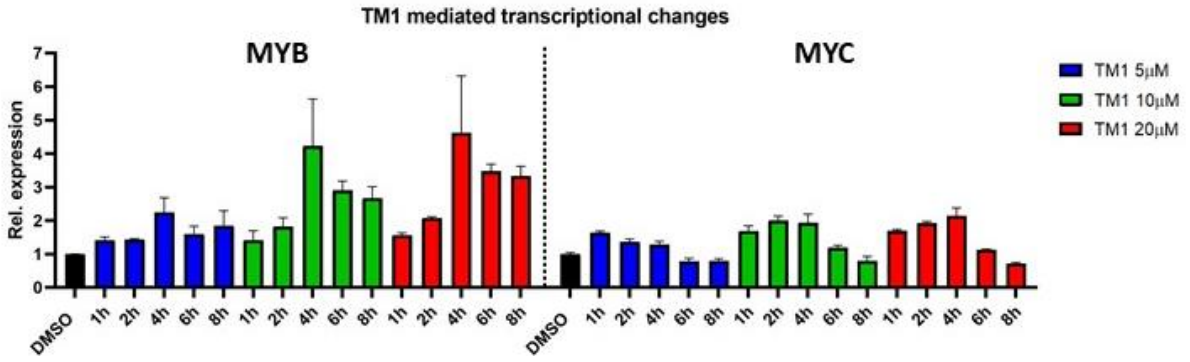

Figure 17: **The effects on TM1 on the relative expression of MYB and MYC,** qPCR based investigation of relative MYB and MYC expression changes after compound exposure, relative fold change calculated by *2^-ΔΔCt*, GAPDH utilized as reference gene, recurring pattern of TM1 mediated effects on MYB expression, x-axis: treatment time in hours, y-axis: relative expression of the investigated gene, bars grouped are based on the investigated gene, left of dashed line: MYB expression, right of dashed line: MYC expression, bars: represent the mean and the standard deviation of biological duplicates in technical triplicates, blue: 5 µM TM1 treatments, green: 10 µM TM1 treatments, red: 20 µM TM1 treatments

After one- and two-hour treatments of TM1 the relative expression of MYB and MYC was slightly increased compared to the control without a noticeable dose dependency. Surprisingly, significant higher MYB expression was observed 4, 6 and 8 hours after the treatment with TM1. The increase is strongest for samples treated with 20 µM TM1 but it was seen for all three doses of TM1. Compellingly, this led to a reoccurring pattern that was most pronounced after 4 hours but was present for the 4, 6 and 8 hours timepoint. Changes in the expression of MYC were less significant. Beside a slight dose dependent decrease at the longest timepoint, MYC was expressed at the same level as the in control. Despite, MYC levels served as important comparison to differentiate between global transcriptional changes and genes specific effects. Intriguingly, the increase in MYB expression contrasted with the stable expression of MYC which suggested a potential MYB specific mechanism.

Another layer of information that was utilized to estimate the effect of TM1 on global transcription is the mRNA level of GAPDH. The cycle threshold values of the housekeeping gene GAPDH, which correlate with the absolute amount of mRNA, did not show an obvious correlation with seen changes in MYB expression. However, due to the design of the performed experiment no absolute reference could be utilized. Thus, fluctuations of GAPDH were not normalized and were influenced by the amount of input RNA. This amount varied because of global transcriptional changes and handling during RNA extraction. Because of that no quantitative analysis of global transcriptional effects could be performed. Instead, the large sample number was utilized to investigate if TM1 and DMSO treatments led to an obvious pattern. The lack of such a pattern in addition to the clear difference between effects on MYB and MYC suggested a gene specific effect.

TM1 induced reduction of c -Myb protein levels was rescued by a co-treatment of the proteasome inhibitor MG132, as shown in figure 15. With the aim to mirror the conditions of the proteome focused experiment and to see if MG132 also abolishes TM1 mediated transcriptional changes, MYB and MYC expression was investigated after co-treatments. Interestingly, TM1 mediated transcriptional changes were very similar for conditions with and without the co-treatment of MG132. The same pattern of a dose dependent increase of MYB expression was observed for both settings. This underlined the significance of observed compound included changes and suggested distinct effect on the transcriptome and proteome.

Summarized, TM1 led to a reoccurring pattern of intriguing transcriptional changes. MYB expression was increase in a dose dependent manner with it´s peak after 4 hours of 20 µM TM1 treatment. Co-treatments of MG132 which rescued TM1 induced reduction of c -Myb levels did not impede TM1´s transcriptional changes significantly. This data supports the initial hypothesis that the seen Myb protein level changes are mediated by post translational mechanisms. Why MYB expression is upregulated remains speculative.

The effects of TM1 on cell proliferation and the induction of apoptosis

To gain a broader understanding of TM1 mediated biological effect its effect in cell viability was investigated. To differentiated between compound mediated induction of apoptosis and senescence. the IncuCyte® (Essen BioScience) Live-Cell Analysis platform with according Caspase 3/7 apoptosis assay was utilized. The platform relays on phase-contrast microscopy and fluorescence microscopy, both performed under optimal cell culture conditions. This allowed to continuously monitor live cell parameters of treated cells. Phase contrast microscopy was used to investigate cell proliferation and the shape of cells. In addition, fluorescence readouts were utilized to monitor the activity of specific pathway, depending on the applied assay. In this case the Caspase 3/7 apoptosis assay was used to measure the induction of apoptosis.

Caspases are a family of proteases that play an essential role in initiation of programmed cell death, apoptosis. Upon activation of the apoptotic pathway, by extracellular or intracellular stimuli, a cascade of caspases is activated. Thereby pro-caspases are proteolytically cleaved into caspases, which activates the protease function and results in additional cleavages of downstream pro-caspases. This leads to a wave like propagation of the signal mediated via proteolytic cleavages that ends in the activation of effector caspases. Caspase 3 and 7 are cysteine proteases with the recognition peptide motif DEVD and are responsible for the executive step of apoptosis, namely major proteolysis. Thus, the activity of caspase 3 and 7 can be measured and utilized as an approximation for apoptosis induction.

The live-cell Caspase 3/ 7 apoptosis assay is based on a peptide that represents the caspase-3/7 recognition motif (DEVD) and a conjugated DNA intercalating dye. The conjugation leads to a non-fluorescent non-DNA binding substrate that can cross the cell membrane of the assay cells. In healthy cells the substrate remains uncleaved due to the inactivity of caspase 3 and 7. Contrasting, cells that undergo apoptosis contain active caspase 3/ 7 which cleaves the substrate and release the fluorescent dye. The dye intercalates into the DNA of the investigated cell and can be measured as fluorescent signal.

Figure 18 depicts a summary of TM1 and MB1 mediated effects on Molt4 viability. The experiment was performed applying the described IncuCyte® (Essen BioScience) Live-Cell Analysis platform with according Caspase 3/7 apoptosis assay. Cell were treated in biological triplicates with DMSO as control or with a dose curve of TM1 or MB1 ranging from 0.625 µM to 40 µM. After the treatment micrographs were continuously taken for 80 hours every three hours. In total more than 2500 pictures were taken in the phase contrast and fluorescence channel. Image processing was performed with the IncuCyte® Analysis Software (Essen BioScience) to retrieve the number of apoptotic cells and confluency of the observed well.

Figure 18a and c shows the mean relative number of apoptotic cells after dose curve treatments of TM1 and MB1, respectively. DMSO controls demonstrated a stable low number of apoptotic cells and were used reference. Figure 18b and d show the mean confluency for each treatment over time. Mean confluency of observed wells was used to normalize the number of apoptotic cells and to differentiate between cytotoxic versus cytostatic compound effects.

High doses of TM1 (5 µM or greater) led to a strong induction of apoptosis during the first 40 hours post treatment, as depicted by figure 18a. Timing and effect size of the induction did show a slight dose dependent variation but was generally very comparable between high TM1 doses. Contrasting, low doses of TM1 (less than 5 µM) did not lead to a significant increase in the number of apoptotic cells during the whole measured period. Consequential a clear difference in TM1 mediated induction of apoptosis can be seen between treatments of higher or lower than 5 µM. This distinction is also seen in TM1´ s effect on cell proliferation. Figure 18b depicts the confluency of DMSO treated wells (red) and TM1 treated wells (black). Mean values with the standard deviation of biological triplicates are presented in the figure. Control wells treated with DMSO showed an expected exponential proliferation with a doubling time of approximately 35 hours. Low dose TM1 treatments (below 5 µM) did not present a considerable influence. In contrast, high dose TM1 treatments (5 µM or higher) impeded the proliferation of Molt4 effectively. No cell proliferation was measured during the whole observation period. A comparison of TM1 mediated effects on cell proliferation and on the induction of apoptosis revealed a very similar pattern with a reoccurring threshold between 2.5 µM and 5 µM.

This suggested that TM1 treatments of 5 µM or higher impede cell proliferation effectively due to the induction of apoptosis. Instead, TM1 treatments of less than 5 µM did not affect cell viability significantly.

In the case of MB1 a different effect on cell viability was observed. MB1 doses of 2,5 µM or higher led to an immediate induction of apoptosis, as seen for TM1. Interestingly, even the lowest doses of MB1 did induce apoptosis starting approximately 20 hours after the treatment. This correlated well with MB1´ s effect in cell proliferation. Even the lowest dose of 0.625 µM led to a significant reduction of cell proliferation.

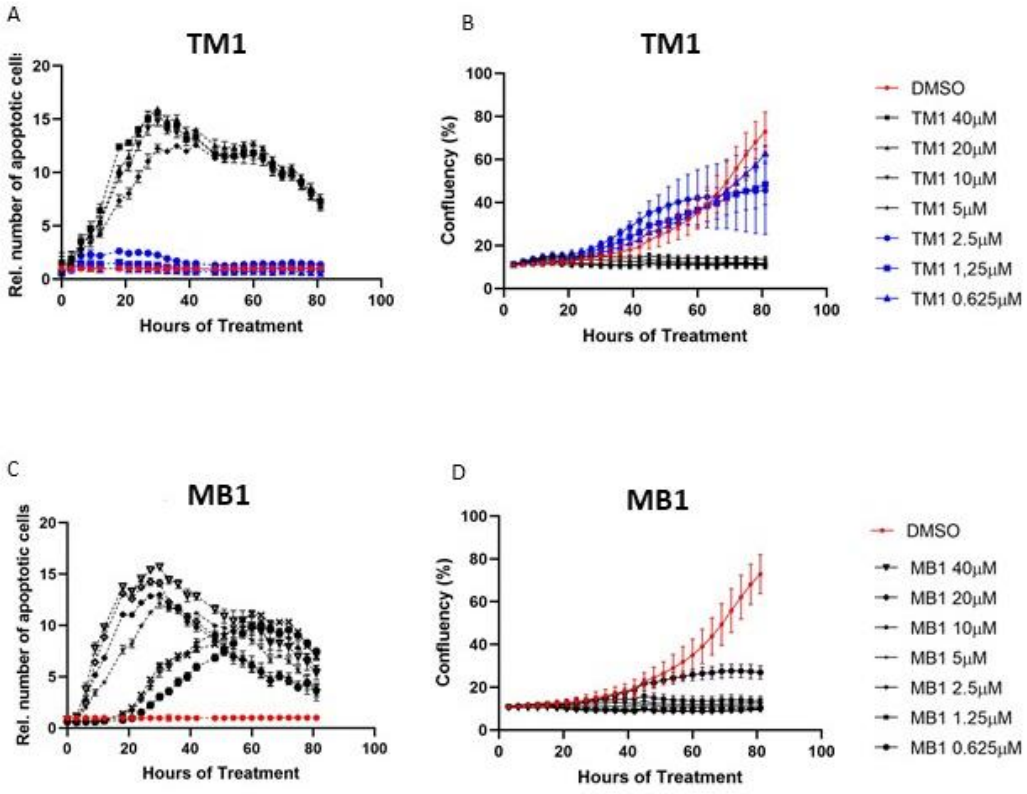

Figure 18: **The effects of TM1 and MB1 on cell proliferation and the induction of apoptosis,** a) the accumulation of apoptotic cells over time after the treatment of TM1, apoptosis induction was measured by detection of caspase-3/7 activity on Molt4, x -axis: hours of treatment, y-axis: the number of apoptotic cells relative to the DMSO control, data points: represent the mean and the standard deviation of biological triplicates, red: DMSO treated cells, blue: TM1 treatments of 2.5 µM or lower, black: TM1 treatments higher than 2.5 µM, exact treatment concentration as depicted in the legend, b) TM1 mediated effect on cell proliferation over time, as measured by confluence as a percent of total available culture area, x -axis: hours of treatment, y-axis: confluency of total culture area in percent, data points: represent the mean and the standard deviation of biological triplicates, treatment conditions: as described for a, c) the accumulation of apoptotic cells over time after the treatment of MB1, treatment conditions: as described for a, red: DMSO, black: MB1 treatments, d) MB1 mediated effect on cell proliferation over time, treatment conditions: as described for a, red: DMSO, black: MB1 treatments

Discussion

Assay choice

The project was initiated with the general aim to discover a small molecule that affects the biology of the TF c-Myb. Building on recent studies that revealed intriguing insights into the biology of c-Myb, the goal was set to find small molecule probes that effect the key PPIs c-Myb : KIX and c-Myb : TAF12. To address this ambitious goal a biochemical assay was of need that provided a reliable tool to screen compounds for their activity against the investigated PPI. The biology of c-Myb´ s regulation is highly complex and still not fully illuminated which made it challenging to design meaningful in vitro assays. Additionally, c-Myb is notoriously difficult to work with which limited the number of potentially applicable assays further. Thus, BRET assays seemed to be the method of choice to find small molecule probes that effect c-Myb´ s interactome. In retrospect, this assumption was strongly supported by two BRET assay features that turned out to be crucial for the success of this study. First, BRET assays are based on an overexpression system in living cells. This provided the opportunity to measure the effect of the applied compound on the investigated PPI while keeping c-Myb in a physiologically relevant setting. Second, BRET readouts are calculated with an internal normalization. This was crucial to explore, if TM1 has an effect on the PPIs of c-Myb or on c-Myb protein levels itself.

BRET assay development

The successful generation of 12 BRET expression construct enabled testing of all potential donor and acceptor combinations. Resulting BRET ratios (Figure 8) provided important insights about potential promising combinations and suggested that both investigated PPIs were applicable for BRET assay development. In addition, measured donor signals of each condition were utilized to estimate the rate of stably expressed fusion protein. Based on that, it was concluded that all three investigated interaction partners were stably expressed in HEK293 cells. Interestingly, Luc-Myb fusion proteins led to the weakest donor signals. This suggested a comparably low protein stability and provided starting points for the optimization of the BRET assay. Surprisingly, high signals were measured for Luc-TAF12 without the co-expression of other HFDs. Based on published data it was expected that co-expression of HFDs would be required for the stability of TAF12. However, this was not observed during the BRET assay development and led to speculations that the fused tag or other factors of the cellular environment stabilized TAF12.

Although the donor signals of measured Luc-fusion proteins could not be directly translated into the amount of Halo tagged fusion proteins, an interesting pattern was revealed. Thus, we hypothesized that Myb fusion proteins are generally less stable compared to KIX or TAF12 fusions. Retrospectively, this would explain why both developed BRET assays yield the highest BRET ratios when performed with

Luc-Myb combined with a Halo tagged interaction partner. Putatively, this combination was most promising to achieve a low donor to acceptor protein quantity ratio. Moreover, low stability of Myb fusion proteins would provide an explanation why shortening of the incubation time after the transfections led to significantly increased BRET ratios. However, hypothesized expression rates and protein stabilities were not further investigated and remain therefore speculative. Despite, important rationales were provided for the successful optimization of both BRET assays. Thus, testing of all fusion protein combinations was a complex but essential step for the successful development of both BRET assay. As a result, we managed to establish stable BRET assays with adequate assay window for c-Myb : KIX and c-Myb : TAF12.

BRET assay application and testing

Verification of the established BRET assays was limited to experiments which utilized BRET specific mechanisms. The reported difference between BRET ratios of developed assays and their according no acceptor controls suggested that both established assays are directly dependent on the investigated PPI. However, no positive controls could be performed because of a lack of published chemical probes with characterized modulation of the investigated PPIs. Thus, it was decided to apply the established BRET assay for screenings in order to find potential modulators and follow with a detailed characterization of found hit compounds.

Excitingly, it was discovered that TM1 led to strong dose dependent reduction of c-Myb : TAF12 BRET ratios (Figure 9). This result was intriguing from the perspective of chemical probe development and assay development. The initial focus was laid on the interpretation of established BRET assays utilizing TM1 mediated changes in observed BRET ratios. Concise, different experiments were performed to investigated if molecular alteration beside the inhibition of the PPI could have led to a decreased BRET ratio. Compellingly, this was not the case. It was shown that neither a compound with putatively acute cytotoxic effects nor a published c-Myb degrader did decrease c-Myb : TAF12 BRET ratios significantly. This emphasized the reported results of TM1 and suggested that the readout of the established BRET assay was specific for the investigated PPI. However, a question that remained unclear is which molecular alterations in c-Myb´s biology or its interactome could modulate the PPI. Based on gathered data and the biophysical principal of BET assays we concluded that other mechanism beside steric blockage of the PPI are feasible. Especially the overexpression system in living cells presents a variety of complexities that could potentially affect the observed BRET ratios. This includes endogenous proteins of HEK293 which could form complexes with the proteins of interest or alter post translational modifications of the overexpressed interactions partners. Consequential, this suggest that compound mediated decrease of BRET ratio correlates with modulation of with the investigated PPI. Despite, this

modulation could be potentially caused by a variety of factors besides steric blockage of the interaction.

Summarized, the developed BRET assays for c-Myb : TAF12 and c-Myb : KIX were successfully optimized and broadly tested. Based on the calculated BRET ratios it was concluded that both assays are directly dependent on the investigated PPI. Thus, optimized BRET assays for c-Myb : TAF12 and c-Myb : KIX could serve as valuable tool for future medium to high throughput screenings aiming to find chemical probes that affect the investigated PPIs.

The discovery and characterization of TM1

TM1 initially emerged as hit compound from a c-Myb focused IVT-based SMM screening. Additionally, it showed promising effects on the activity of c-Myb in a reporter gene assay and was therefore prioritized for further development.

The effect of TM1 on c -Myb´ s interactome

Our success to establish BRET assay for c-Myb : TAF12 and c-Myb : KIX provided the opportunity to test compounds for their ability to modulate the investigated PPIs. TM1 caused a strong dose dependent reduction of c-Myb : TAF12 BRET ratios with an IC50 of approximately 7 µM (Figure 8). In contrast, weak changes were observed in the case of c-Myb : KIX and no effects on the PPI of an unrelated BRET assay positive control. Thus, we concluded that TM1 is a putative modulator of c-Myb : TAF12 that has no significant impact on BRET assays *per se*. Observed effects on the interaction of c-Myb : KIX were more difficult to interpret. We hypothesized that weak BRET assay changes might be caused by destabilization of the investigated protein complex or structural rearrangements. Building on the insights of published studies which solved the structure of c-Myb : KIX, we speculated that two molecular alterations that involve TAF12 potentially led to destabilization of the interaction [29]. Either the disruption of the PPI between c-Myb and TAF12 itself or an unknown mechanism which led to the disruption of c-Myb : TAF12, could affected c-Myb : KIX. The described explanations remained speculative. Nevertheless, it was intriguing for us to see that TM1 affected both interactions at an IC50 concentration of approximately 7 µM, which is noteworthy very similar to reported IC50 centration of the reporter gene assay. This emphasized that TM1 has an effect on c-Myb´ s biology and suggested potentially selective modulation of c-Myb : TAF12. Importantly, modulation of the PPI could be caused by steric blockage but also by a variety of other mode of actions including compound mediated alteration of c-Myb´ s post translational modifications.

Biological effects of TM1

TM1 treatments caused a rapid dose dependent reduction of c-Myb protein levels whereas mRNA levels were significantly increased. The protein level reduction followed an exponential decay and was

rescued by a co-treatment of a proteasome inhibitor. Based on that, we concluded that TM1 led to proteasome mediated degradation of c-Myb with an EC50 value of approximately 5 µM. This was especially interesting because of published data which suggested that the stability of c-Myb is dependent on TAF12. Thus, the observed degradation of c-Myb and the proposed TM1 mediated modulation of c-Myb : TAF12 at comparable IC50 and EC50 values, were highly intriguing. However, it has to be mentioned that the exact mechanism how TM1 led to proteasome mediated degradation remained unclear. We speculated that steric blockage of c-Myb : TAF12 or compound mediated alterations of c-Myb´ s post translational modifications could have led to observed results. Unbiased proteomics *via* the application of mass spectrometry would be required to investigation global changes in the proteome or alterations in c-Myb´ s post translational modifications.

The qPCR-based investigation of TM1 mediated effects on the transcriptome revealed unexpected relative expression changes. MYB expression was significantly increased after cells were exposed to TM1 for 4 hours. Whereas, the relative expression of c-Myb target genes, MYC and presumably CCNB1, was not significantly affected by TM1 treatments (Figure 17). The distinct effects of TM1 on c-Myb protein levels and mRNA levels were striking to us because of two reasons. First, observed results supported the hypothesis that TM1 mediated protein level changes were based on post translational mechanisms. Second, TM1 mediated increase of MYB gene expression suggested the potential presence of cellular mechanisms which compensate the degradation of c-Myb. Moreover, TM1 induced transcriptional changes occurred in the absence and presence of a proteasome inhibitor, which recused the degradation of c-Myb. Thus, we concluded that the “protein level rescue” prevented the degradation of c-Myb but did not impede the mode of action of TM1. In other words, this would suggest that the co-treatment of a proteasome inhibitor led to accumulation of nonfunctional c-Myb which provides another interesting link to the hypothesized involvement of post translational modifications. Yet, it was unclear why TM1 did not affect c-Myb target genes significantly. Additionally, considering the essential role of TFIID for global transcription, concerns were raised that reported relative expression changes missed global transcriptional effects. Despite the mRNA amount of the reference gene did not show an obvious correlation with TM1 treatments, global transcriptional effects could not be assessed with the performed assay. To address this question and to investigate TM1 mediated transcriptional changes in more depth, unbiased transcriptional profiling utilizing RNA sequencing with spike in controls, would be required.

To complement the picture of TM1 mediated biological effects, its influence on cellular viability was investigated. Strikingly, initial experiments revealed that TM1 lead to decreased cell viability of human T lymphocytes. In order to establish dose dependency and to distinguish between induction of apoptosis and senescence a Live-Cell Analysis platform was applied. Summarized, rapid induction of

apoptosis was observed for TM1 treatments with a threshold between 2.5 µM and 5 µM. No significant effect on cell proliferation or apoptosis induction were observed for TM1 treatments below 2.5 µM. This experiment confirmed that TM1 led to cancer cell death by the induction of apoptosis. Moreover, it revealed that compound mediated effects on cell viability had a sharp threshold between 2.5 µM and 5 µM, which was in a similar concentration range as reported IC50 and EC50 concentrations of c-Myb : TAF12 modulation and c-Myb degradation, respectively. This was striking to us since it suggested that the observed induction of apoptosis is potentially in direct correlation with the modulation of c-Myb : TAF12. Minor deviations in reported IC50 and EC50 concentration could be potentially caused by assay specific properties or by the range of utilized assay read outs.

Summarized, gained insights into compound mediated biological effects suggest that TM1 is a putative modulator of c-Myb : TAF12 which leads to potent anti-cancer effect, including the induction of apoptosis and proteasome mediated degradation of c-Myb.

Potential mode of action and future development of TM1

Presented insights suggest that post translational modification of c-Myb play an essential role in TM1´ s mode of action. However, if these alterations are a result or the cause of c-Myb : TAF12 destabilization remains speculative. Thus, TM1 could act *via* a variety of molecular mechanisms including steric blockage of the PPI and inhibition of post translational modification modifying enzymes. Unbiased investigation of global transcriptional effects, global changes of post translational modifications and target engagement will be required for the understanding TM1´ s mode of action. In addition, CRISPR screenings could be a valuable tool to find molecular pathways that are essential for the mode of action of TM1.

Methods

Standard cloning procedures

Primer design and In-silico cloning

Primer design and in – silico cloning were performed with Snapgene® (version 5.1). The Melting - Temperature (Tm) of complimentary sequence parts of designed primers was calculated with NEB® Tm calculator (version 1.12.0). Investigation for possible self – complimentary or hairpin formation was done with mfold [55]. In-silico cloning mirrored the designed cloning strategy in order to ensure successful plasmid generation.

Standard PCR

PCR - Reactions were performed with NEBNext® High-Fidelity 2x PCR Master Mix (M0541) according to manufacturer protocol. Short, a 50 µL reaction consisted of 25 µL master mix, 2.5 µL of each primer

(final concentration 0.5 µM), 1 µL of template DNA and 19 µL ddH_2O. Standard cycling conditions were an initial denaturation step (98 °C, 30 s), 25 amplification cycles with a denaturation - step (98 °C, 10 s), an annealing – step at different temperatures depending on the used primers (Tm -3 °C, Tm, Tm + 3 °C, 30 s), and an extension - step (72 °C, 1 min) followed by a final extension - step (72 °C, 2 min). A small amount of the reaction product was examined on a 1,5% agarose gels. SYRB safe DNA gel stain and ChemiDoc™ imaging system (BioRad) were used to visualize bands on the gel and estimate the according sequence length.

PCR purification

All PCR purifications were carried out with a silica-membrane-based Quiagen kit (cat. no. 28104). Purifications were performed according to manufacturer handbook. To determine DNA concentration NanoDrop 2000 UV – Vis Spectrometer (Thermo scientific) was used.

Restriction digest

For all digests restriction enzymes from NEB® were used. Plasmid digests were carried out according to manufacturer protocol. The components for 20 µL digests were 2 µL 10x CutSmart® Buffer (NEB®), 500 ng of PCR product or 1 µg of plasmid DNA, 1 µL of each enzyme (according to used sequences) and ddH_2O to a final volume of 20 µL. Reactions were incubated for 2 h at 37 °C to perform the digest. Subsequently, reactions were inactivated by 75 °C for 10 min. In case of analytical digests, the resulting product was examined on a 1,5 % agarose gel. SYRB safe DNA gel stain and ChemiDoc™ imaging system (BioRad) were used to visualize bands on the gel and estimate the according sequence length.

Gel extraction

The Macherey-Nagel™ gel extraction kit (REF 740609.50) was used to carry out all gel extractions. Therefore, a vector digest was applied to a 1,5 % agarose gel. Gel - electrophoreses was performed for 60 min at 120 volts to separate DNA bands. Resulting bands were excised from the gel and applied as starting material for the kit. Purification was performed according to manufacturer protocol. To determine the DNA concentration of the resulting elution, NanoDrop 2000 UV – Vis Spectrometer (Thermo scientific) was used.

Ligation

All ligations were performed with purchased T4 DNA Ligase from NEB® (cat. no. M0202T) Ligations were done in 20 µL reactions, containing 1 unit T4 Ligase, 2 µL 10x T4 Ligase Buffer (NEB®) and varying amounts of inserts and vectors, depending on the specific application, and ddH_2O to a final volume of 20 µL. The reactions were incubated at 17 °C over night, followed by an inactivation at 65 °C for 10 min.

Transformation

NEB® 5-alpha competent *E. coli* cells were used for all transformations. 50 µL high competent cells were mixed with 1 µL DNA solution. The mixture was incubated on ice for 30 min, heat shocked at 42 °C for 30 s and cooled down on ice for 5 min. Transformed cells were mixed with 950 µL SOC medium and incubated at 37 °C for 30 min for recovery. Afterwards the whole transformation mixture was plated on LB – Agar plates containing the according antibiotic.

Plasmid DNA isolation from *E. coli* (small scale)

To obtain purified plasmid, precultures of desired colonies were prepared. Therefore, 5 ml of LB-media with the according antibiotic were inoculated with a small amount of the desired *E. coli* colony and incubated at 37 °C over night. Cells were harvested and plasmids were extracted using the QIAprep Spin Miniprep Kit (Qiagen). Extraction was performed according to the manufacturer handbook.

Sequencing

All samples were sequenced using the Quintarabio´ s Sanger sequencing service. For sample preparation 10 µL purified plasmid (concentration 100 ng μL^{-1}) were mixed with 5 µL sequencing primer. Sequencing – results were analyzed with Snapgene® (version 5.1) and Ncbi BLAST.

BRET assays construct generation

BRET constructs were generated utilizing the Flexi® Cloning System (Promega Corporation) according to manufacturer protocol. Each open reading frame (ORF) of interest (c-Myb, TAF12, KIX) was cloned into the entry vector pFN21A using the restriction enzymes PmeI and AsiSI. Therefore, ORFs were amplified and purified using *standard PCR* and *PCR purification* as described previously. Applied forward and reverse primers contained overhangs with the restriction enzyme cutting site for PmeI and AsiSI, respectively. The PCR products and the entry vector were digested with PmeI and AsiSI according to previously described *restriction digest.* Digested PCR products were purified according to *PCR purification*. 50 ng digested vector and 100 ng digested and purified PCR product were then ligated and used for transformation of competent *E. coli* as described in the paragraph *ligation* and *transformation*, respectively. LB – agar plates (+ carbenicillin 100 µg mL^{-1}) with transformed *E.coli* cells were incubated at 37 °C over night. 5 colonies of each transformation were further investigated by analytical digests with PmeI and AsiSI. Plasmids of promising colonies were then sequenced as described in *sequencing.* After successful generation of pFN21A vectors with each ORF of interest, inserts were transferred to remaining BRET vectors. In case of the vector pFN31K (acceptor construct), inserts were transferred utilizing the restriction enzymes PmeI and AsiSI in combination with pFN21A constructs (donor). Therefore, 100 ng of acceptor and donor construct with cloned ORFs, were digested with PmeI and AsiSI, according to *restriction digest.* 50 ng of each digest were then used for

ligation and transformation of competent *E. coli*, as described previously. LB – agar plates (+ kanamycin 50 µg mL^{-1}) with transformed *E.coli* cells were incubated at 37 °C over night. Obtained colonies were handled as described to verify successful generation of the desired construct. In case of the vectors pFC14K and pFC32K, the orientation of the tag had to be changed from N to C-terminal. Thus, two different sets of restriction enzymes were used for the digest of the donor and acceptor constructs to omit the stop codon of the donor construct. Therefore, 100 ng of pFC14K and pFC32K were digested with PmeI and EcoICRI. In addition, 100 ng of the donor construct pFN31A (+ cloned ORF) were digested with PmeI and AsiSI, according to *restriction digest.* 50 ng of each digest were then used for ligation and transformation of competent *E. coli*, as described previously. LB – agar plates (+ kanamycin 50 µg mL^{-1}) with transformed *E.coli* cells were incubated at 37 °C over night. Obtained colonies were handled as described to verify successful generation of the desired constructs.

Plasmid DNA isolation from *E. coli* (large scale)

To obtain purified plasmid for the implementation of BRET assays, precultures of desired *E. coli* cells were prepared. Therefore, 5 ml of LB-media with the according antibiotic were inoculated with a small amount of the *E. coli* cells (picked form an LB-agar plate or glycerol stock) and incubated at 37 °C over night. The preculture was added to 50 ml LB-media with the according antibiotic that was prewarmed to 37 °C. Cultures were then incubated for 24 h at 37 °C. Cells were harvested and plasmids were extracted using the QIAprep Spin Midiprep Kit (Qiagen). Extraction and endotoxin removal were performed according to the manufacturer handbook.

BRET assays development

All BRET assays were performed according to the manufacturer protocol. In detail, HEK293 cells with a passaging number lower than 25, were cultured in DMEM media with 5% FBS under optimal cell culture conditions (37 °C, 5% CO_2) for at least a week previous to the assay. For assay cell preparation the cells were washed with PBS, detached by the addition of trypsin and resuspended in DMEM media with 5% FBS. 260 000 cells were plated per well of a 12 well coated tissue culture plate. Cells were incubated under optimal conditions for 9 h to ensure recovery. Subsequently, cells were transfected with different BRET constructs utilizing FuGene® 6 (Promega Corporation) as transfection reagent. Therefore, 50 µL Opti-MEM ® Reduced Serum Medium without phenol red were mixed with 6 µL FuGene® 6 and the according amounts of expression plasmid. For the transfection control 1 µg of pcDNA with a GFP expression cassette was used. In case of cells that were prepared for BRET assays, 1 µg of according HaloTag® plasmid and 0.1 µg of NanoLuc® plasmid were utilized. Except the BRET assay positive control were 0.01 µg of NanoLuc® plasmid were used. All mixtures were then incubated for 15 min at RT and subsequently added to the recovered cells in dropwise manner. Cells were incubated under optimal conditions for 24 h to ensure expression of the transfected plasmids. Cells

were then washed with PBS, detached by the addition of trypsin and resuspended in Opti-MEM media with 4% FBS (assay media). Cells were centrifuged for 5 min at 300 g to remove inactivated trypsin and resuspended in assay media with DMSO or HaloTag at 100 nM final concentration. 20 000 cells of each transfection condition were plated per well of 96-well tissue culture plate in the presence and absence of HaloTag, by adding 100 µL of a 200 000 cell/mL cell suspension to each well. Assay cells were then incubated at 37 °C for 18 h and at RT for 30 min prior to the BRET assay measurement. Subsequently, 25 µl of substrate solution (Opti-MEM + 100x dilution of provided substrate stock) were added and plates were shacked for 30 sec to ensure mixing. BRET measurements were performed with the PerkinElmer® EnVision® platform according to recommended instrument settings. Filter "Umbelliferone 460" and filter "Cy3 595" were used to measure the donor and acceptor signal, respectively. Calculation of BRET ratios were performed according to the manufacturer protocol and as described previously.

BRET assay optimization

Optimized BRET assays were performed as previously described in paragraph *BRET assays development*, except following deviations. BRET assay cells were transfected in 6-well tissues culture plates or T-175 tissue culture flasks. Therefore, the amounts of used reagents and cells were increased according to the surface area of the used tissue culture plate or flask. In addition, plasmids form large scale preparation were used for the transfection. Incubation of transfected cells was decreased from 24 h to 12 h. Subsequently, cells were replated as described. Cell were then incubated at 37 °C for 5.5 h and at RT for 30 min prior to the BRET assay measurement.

BRET assay dose curves

Application of optimized BRET assays for compound testing was performed as described in paragraph *BRET assay optimization*, except the replating procedure. In detailed, 20 000 assay cells were plated per well of a 96-well tissue culture plate in the presence of 200 nM HaloTag, by adding 50 µL of a 400 000 cell/mL cell suspension to each well. Subsequently, cells were treated by the addition of 50 µL assay media with DMSO or compound dissolved in DMSO at the appropriate final concentration. Cells were then incubated at 37 °C for 5.5 h and at RT for 30 min prior to the BRET assay measurement.

Cell titer glow measurements

Molt4 cells were plated in 96-well plates, by adding 50 µL of a 200 000 cell/mL cell suspension in RPMI media to each well. Subsequently, cells were treated by the addition of 50 µL RPMI media with DMSO or compound dissolved in DMSO at the appropriate final concentration.. After the cells were incubated at 37 °C for the specified treatment time, 100 µL of CellTiter-Glo® reagent (Promega Corporation) were

added to each well. Plates were agitated for 10 min and measured utilizing an Infinite 200 Pro (Tecan Life Sciences) plate reader.

Quantitative western blotting

Molt4 cells were plated in 12-well plates, by adding 2 ml of a $1*10^6$ cell/mL cell suspension in RPMI media to each well. Cell were treated with DMSO or compound dissolved in DMSO at the appropriate final concentration for 6 h, unless specified. Subsequently, cells were harvested by centrifugation (300 g, 5 min) and washed with ice-cold PBS. Cell lysis was performed with 4x volume of RIPA buffer (Thermo Fischer Scientific) supplemented with 1x cOmplete™ protease inhibitor cocktail and 1x PhosSTOP™ (both Sigma Aldrich). Lysates were centrifuged for 20 minutes at 4 °C to remove cell debris. Concentration of total protein was measured *via* BCA protein assay kit (cat. no. 71285 71285 M) and adjusted to with ddH_2O to 1 mg/mL. Subsequently, samples were prepared for electrophoresis by heating to 90 ˚C for 5 min in a final concentration of 1x Laemmli loading buffer (supplemented with 5% beta-mercaptoethanol, freshly added). Samples were then resolved by SDS-PAGE (4–15% Criterion™ TGX™ Precast gel, BioRad) at a constant voltage within the range of 160 – 200 V. Proteins were transferred to a nitrocellulose membrane (BioRad) using the Trans-Blot® Turbo™ transfer system from BioRad. Membranes were blocked with 5% BSA in TBS-T for a minimum of 1 hour (RT) before incubating with the primary antibodies (c-Myb antibody (12319, Cell Signalling Technology), TAF12 antibody (ab229487, abcam), H3 antibody (9715, Cell Signalling Technology)). Membranes were washed 3 times with TBS -T for 5 min before secondary antibodies were applied. Either anti-mouse or anti-rabbit HRP linked antibodies (BioRad) were incubated with the membrane for 45 min. Membranes were washed 3 times with TBS -T for 5 min before imaging on a ChemiDoc™ imaging system (BioRad) was performed according to manufacturer protocol.

IncuCyte® live cell assay

Molt4 cells were plated in 96-well plates (coated with Fibronectin 5 µg/ml) by adding 50 µL of a $1*10^6$ cell/mL cell suspension in assay media to each well. The assay media contained 10 µM of IncuCyte® Caspase-3/7 Green Apoptosis Assay Reagent (Essen Biosciences) according to manufacturer protocol. Subsequently, cells were treated by the addition of 50 µL RPMI media with DMSO or compound dissolved in DMSO at the appropriate final concentration. Plates were then imaged over an 80-hour period, collecting 4 images per well every 3 hours with a 10x objective using the IncuCyte® S3 in a standard tissue culture incubator. The resultant images were analyzed for confluency and apoptotic signal using the associated IncuCyte® S3 software, adjusting the mask and filter settings for image analysis.

RT-qPCR Studies

Molt4 cells were plated in 96-well plates, by adding 180 µL of a 1,25*10^6 cell/mL cell suspension in RPMI media to each well. Cells were treated by the addition of 20 µL RPMI media with DMSO or compound dissolved in DMSO at the appropriate final concentration. At the end of the treatment cells were transferred to 96-well V-shape plates and spun down at 300 g for 5 min. Cells were washed in PBS and the RNA was extracted and purified using the Direct-zol-96 RNA kit (Cat. No. R2054, ZYMO Research) according to manufacturer protocol. High-Capacity cDNA Reverse Transcription Kit (Life Technologies) was applied according to manufacturer protocol to generate cDNA libraries from each sample. Specific transcripts were quantified by qPCR using the TaqMan Fast Advanced Master Mix (Life Technologies) with FAM-labelled TaqMan probes for GAPDH (Hs99999905_m1) and VIC-labelled TaqMan probes for MYB (Hs00920556_m1) and MYC (Hs00153408_m1) on a BioRad CFX qPCR instrument compatible with 384-well plates.

References

1. Cramer, P. Organization and regulation of gene transcription. *Nature* **573,** 45–54 (2019).
2. Alberts, B. *Molecular biology of the cell.* 4th ed. (Garland Science, New York, NY, 2002).
3. Lambert, S.A. *et al.* The Human Transcription Factors. *Cell* **172,** 650–665 (2018).
4. Zhou, Y. & Ness, S.A. Myb proteins: angels and demons in normal and transformed cells **2013** (2013).
5. Ness, S.A. The Myb oncoprotein: regulating a regulator. *Biochimica et biophysica acta* **1996** (1996).
6. George, O.L. & Ness, S.A. Situational awareness: regulation of the myb transcription factor in differentiation, the cell cycle and oncogenesis. *Cancers* **6,** 2049–2071 (2014).
7. Corradini, F. *et al.* Enhanced proliferative potential of hematopoietic cells expressing degradation-resistant c-Myb mutants. *The Journal of biological chemistry* **280,** 30254–30262 (2005).
8. Ganter, B. & Lipsick, J.S. Myb and oncogenesis. *Advances in cancer research* **76,** 21–60 (1999).
9. Introna, M. & Golay, J. How can oncogenic transcription factors cause cancer: a critical review of the myb story. *Leukemia* **13,** 1301–1306 (1999).
10. Tsherniak, A. *et al.* Defining a Cancer Dependency Map. *Cell* **170,** 564-576.e16 (2017).

11. Zuber, J. *et al.* An integrated approach to dissecting oncogene addiction implicates a Myb-coordinated self-renewal program as essential for leukemia maintenance. *Genes & development* **25,** 1628–1640 (2011).

12. Xu, Y. *et al.* A TFIID-SAGA Perturbation that Targets MYB and Suppresses Acute Myeloid Leukemia. *Cancer cell* **33,** 13-28.e8 (2018).

13. Doyle, S.K., Pop, M.S., Evans, H.L. & Koehler, A.N. Advances in discovering small molecules to probe protein function in a systems context. *Current opinion in chemical biology* **30,** 28–36 (2016).

14. Dang, C.V., Reddy, E.P., Shokat, K.M. & Soucek, L. Drugging the 'undruggable' cancer targets. *Nature reviews. Cancer* **17,** 502–508 (2017).

15. James Barsoum. Drugging the Undruggable: Transcription Factors. Viewpoint. *Viewpoint* (2017).

16. Orphanides, G., Lagrange, T. & Reinberg, D. The general transcription factors of RNA polymerase II. *Genes & development* **10,** 2657–2683 (1996).

17. Martinez, E. Multi-protein complexes in eukaryotic gene transcription. *Plant molecular biology* **50,** 925–947 (2002).

18. Vaquerizas, J.M., Kummerfeld, S.K., Teichmann, S.A. & Luscombe, N.M. A census of human transcription factors: function, expression and evolution. *Nature reviews. Genetics* **10,** 252–263 (2009).

19. Ibanez, C.E. & Lipsick, J.S. Structural and functional domains of the myb oncogene: requirements for nuclear transport, myeloid transformation, and colony formation. *Journal of virology* **62,** 1981–1988 (1988).

20. Burley, S.K. & Roeder, R.G. Biochemistry and structural biology of transcription factor IID (TFIID). *Annual review of biochemistry* **65,** 769–799 (1996).

21. Gordân, R., Hartemink, A.J. & Bulyk, M.L. Distinguishing direct versus indirect transcription factor–DNA interactions. *Genome Research* **19,** 2090–2100 (2009).

22. Fontaine, F., Overman, J. & François, M. Pharmacological manipulation of transcription factor protein-protein interactions: opportunities and obstacles. *Cell regeneration (London, England)* **4,** 2 (2015).

23. Schilbach, S. *et al.* Structures of transcription pre-initiation complex with TFIIH and Mediator. *Nature* **551,** 204–209 (2017).

24. Vanja Haberle & Alexander Stark. Eukaryotic core promoters and the functional basis of transcription initiation. *Nat Rev Mol Cell Biol* **19,** 621–637, https://www.nature.com/articles/s41580-018-0028-8 (2018).

25. Arkin, M.R., Tang, Y. & Wells, J.A. Small-molecule inhibitors of protein-protein interactions: progressing toward the reality. *Chemistry & biology* **21,** 1102–1114 (2014).

26. Myb proteins: angels and demons in normal and transformed cells (2011).

27. Karl-Heinz Klempnauer, Geoff Symonds, Gerard I. Evan & J. Michael Bishop. Subcellular localization of proteins encoded by oncogenes of avian myeloblastosis virus and avian leukemia virus E26 and by the chicken c-myb gene. *Cell* **37,** 537–547, https://www.cell.com/cell/pdf/0092-8674(84)90384-2.pdf?_returnURL=https%3A%2F%2Flinkinghub.elsevier.com%2Fretrieve%2Fpii%2F0092867484903842%3Fshowall%3Dtrue (1984).

28. Zor, T., Guzman, R.N. de, Dyson, H.J. & Wright, P.E. Solution structure of the KIX domain of CBP bound to the transactivation domain of c-Myb. *Journal of molecular biology* **337,** 521–534 (2004).

29. Zor, T., Mayr, B.M., Dyson, H.J., Montminy, M.R. & Wright, P.E. Roles of phosphorylation and helix propensity in the binding of the KIX domain of CREB-binding protein by constitutive (c-Myb) and inducible (CREB) activators. *The Journal of biological chemistry* **277,** 42241–42248 (2002).

30. Howe, K.M. & Watson, R.J. Nucleotide preferences in sequence-specific recognition of DNA by c-myb protein. *Nucleic acids research* **19,** 3913–3919 (1991).

31. Lipsick, J.S. & Baluda, M.A. The myb oncogene. *Gene amplification and analysis* **4,** 73–98 (1986).

32. Srivastava, S.K. *et al.* Myb overexpression overrides androgen depletion-induced cell cycle arrest and apoptosis in prostate cancer cells, and confers aggressive malignant traits: potential role in castration resistance. *Carcinogenesis* **33,** 1149–1157 (2012).

33. Tomita, A. *et al.* c-Myb acetylation at the carboxyl-terminal conserved domain by transcriptional co-activator p300. *Oncogene* **19,** 444–451 (2000).

34. Ramsay, R.G. & Gonda, T.J. MYB function in normal and cancer cells. *Nature reviews. Cancer* **8,** 523–534 (2008).

35. Pattabiraman, D.R. *et al.* Interaction of c-Myb with p300 is required for the induction of acute myeloid leukemia (AML) by human AML oncogenes. *Blood* **123,** 2682–2690 (2014).

36. Dai, P. *et al.* CBP as a transcriptional coactivator of c-Myb. *Genes & development* **10,** 528–540 (1996).

37. Ho Man Chan and Nicholas B. La Thangue. p300/CBP proteins: HATs for transcriptional bridges and scaffolds.

38. Oelgeschläger, M., Janknecht, R., Krieg, J., Schreek, S. & Lüscher, B. Interaction of the co-activator CBP with Myb proteins: effects on Myb-specific transactivation and on the cooperativity with NF-M. *The EMBO Journal* **15,** 2771–2780 (1996).

39. Stelloo, S. *et al.* Endogenous androgen receptor proteomic profiling reveals genomic subcomplex involved in prostate tumorigenesis. *Oncogene* **37,** 313–322 (2018).

40. Koehler, A.N. A complex task? Direct modulation of transcription factors with small molecules. *Current opinion in chemical biology* **14,** 331–340 (2010).

41. Lambert, M., Jambon, S., Depauw, S. & David-Cordonnier, M.-H. Targeting Transcription Factors for Cancer Treatment. *Molecules : A Journal of Synthetic Chemistry and Natural Product Chemistry* **23** (2018).

42. Bhagwat, A.S. & Vakoc, C.R. Targeting Transcription Factors in Cancer. *Trends in cancer* **1,** 53–65 (2015).

43. Zhang, Y., Cao, H. & Liu, Z. Binding cavities and druggability of intrinsically disordered proteins. *Protein science : a publication of the Protein Society* **24,** 688–705 (2015).

44. Bushweller, J.H. Targeting transcription factors in cancer - from undruggable to reality. *Nature reviews. Cancer* **19,** 611–624 (2019).

45. Zhang, Z. *et al.* Chemical perturbation of an intrinsically disordered region of TFIID distinguishes two modes of transcription initiation. *eLife* **4** (2015).

46. Bradner, J.E. *et al.* A robust small-molecule microarray platform for screening cell lysates. *Chemistry & biology* **13,** 493–504 (2006).

47. Pop, M.S., Wassaf, D. & Koehler, A.N. Probing small-molecule microarrays with tagged proteins in cell lysates. *Current protocols in chemical biology* **6,** 209–220 (2014).

48. Kronos Bio. Our science. Available at https://kronosbio.com/home/our-science-page/#small-molecule-anchor (2020).

49. Struntz, N.B. *et al.* Stabilization of the Max Homodimer with a Small Molecule Attenuates Myc-Driven Transcription. *Cell chemical biology* **26,** 711-723.e14 (2019).

50. Pfleger, K.D.G. & Eidne, K.A. Illuminating insights into protein-protein interactions using bioluminescence resonance energy transfer (BRET). *Nature methods* **3,** 165–174 (2006).

51. Wu, P. & Brand, L. Resonance energy transfer: methods and applications. *Analytical biochemistry* **218,** 1–13 (1994).

52. Coriano, C., Powell, E. & Xu, W. Monitoring Ligand-Activated Protein-Protein Interactions Using Bioluminescent Resonance Energy Transfer (BRET) Assay. *Methods in molecular biology (Clifton, N.J.)* **1473,** 3–15 (2016).

53. Machleidt, T. *et al.* NanoBRET--A Novel BRET Platform for the Analysis of Protein-Protein Interactions. *ACS chemical biology* **10,** 1797–1804 (2015).

54. Thul, P.J. *et al.* A subcellular map of the human proteome. *Science (New York, N.Y.)* **356** (2017).

55. Zuker, M. Mfold web server for nucleic acid folding and hybridization prediction. *Nucleic acids research* **31,** 3406–3415 (2003).

Acknowledgement

First of all, I would like to say thank you to Angela Koehler, the principal investigator of the research group. She allowed me to plan and conduct my own research project in her lab. Furthermore, she supported my research and my carrier plan in many different ways. A special thank you goes to Jasmin Kruell, André Richters, Shelby Doyle and Becky Leifer, who were part of the research group and were my mentors during my stay at MIT. Further I would like to say thank you to all other group members of the Koehler Lab for answering all my questions and being very welcome to me. In addition, I am gratefully for the help of all collaboration partner. Especially, thank you to Amedeo Vetere from the Broad Institute, Chris Vakoc from the Cold Spring Harbor Laboratory and Kimberly Stegmaier from the Dana-Farber Cancer Institute. Another thank you goes to the FH Campus Vienna, my home university, for training me and allowing me to study abroad. A big thank you goes thereby to Susanne Zhanial, the international coordinator of the FH Campus Wien, for helping me with completion of organizational procedures. A special thank you goes also to the Austrian Marshall Plan Foundation for providing financial support which enabled me to conduct this research project abroad. In the end, I would like to express my gratefulness to my family and to my friends for supporting me in many different ways.